SEP 30 1963

DTIE

MASTER

GEMP-219
(Informal)

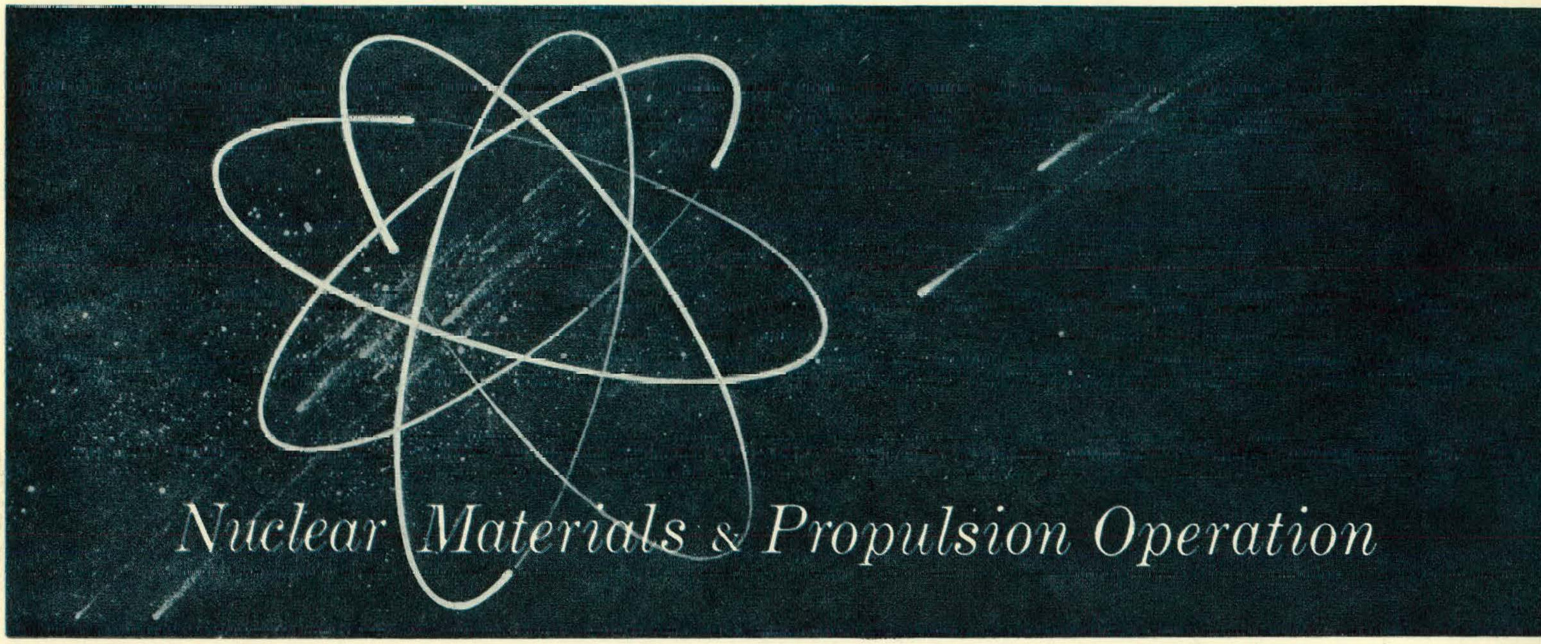

THE SINTERING OF BeO TO VARIABLE DENSITIES AND GRAIN SIZES

E. C. Duderstadt
J. F. White

September 1963

ADVANCED TECHNOLOGY SERVICES

[redacted]

GENERAL ELECTRIC

LEGAL NOTICE

GEMP-219
(Informal)

THE SINTERING OF BeO TO VARIABLE DENSITIES AND GRAIN SIZES

E. C. Duderstadt
J. F. White

September 1963

United States Atomic Energy Commission Contract No. AT (40-1)-2847

Nuclear Materials and Propulsion Operation
Advanced Technology Services
GENERAL ELECTRIC COMPANY

Cincinnati 15, Ohio

DISTRIBUTION

EA Aitken
WG Baxter
JR Beeler
HC Brassfield
VP Calkins
BA Chandler
CG Collins
JF Collins
PK Conn
JB Conway
EC Duderstadt (10)
HS Edwards
EW Filer
R Fryxell
JA McGurty
J Moteff
GT Muehlenkamp
FC Robertshaw
PP Turner
JF White(15)
Reports Library (3)
CL Chase

DTIE

ABSTRACT

This work describes the preparation of BeO samples for a study of the effects of irradiation including the influence of purity, additives, porosity, and grain size. These samples were prepared from three commercially available grades of BeO using extrusion and sintering as the main means of fabrication. One grade of BeO contained some long needle like particles and preferred orientation was observed in extruded samples from this material.

The sintering behavior generally followed the normally observed characteristics. Low density material, prepared by adding an organic material, however, showed the predicted behavior expected from the presence of pores about 10 microns in diameter.

The BeO powder characteristics are given along with the sintering data and photomicrographs of typical samples. The grain growth versus time at temperature for densities of 2.60, 2.75 and 2.95 gms/cm^3 are shown for grain sizes up to 100 microns.

INTRODUCTION

Sintered BeO samples with a variety of microstructures were required for a study to define the physical and mechanical properties of irradiated BeO as they are influenced by purity, additives, and porosity at various irradiation temperatures and dosages. Samples were prepared from three commercially available grades of beryllium oxide or hydroxide. Two of the grades were modified by minor additions of MgO or ZrO_2 to provide a total of six compositions. The desired densities were 2.60, 2.75, and 2.90 g/cm^3 with various grain sizes up to 100 microns in diameter.

This report catalogues the raw materials, briefly describes the isostatic pressing and extrusion processes, describes the sintering of the BeO samples, and contains an evaluation of the sintering data. These latter data were examined to determine the significant effects of composition differences, sintering time and temperature variations, and process variables which were introduced to obtain the required microstructure variations.

RAW MATERIALS

Three grades (or types) of BeO were used in this study:

(a) UOX grade from the Brush Beryllium Company which is prepared from a sulfate and is of relatively high purity.

(b) AOX grade from the Brush Beryllium Company which is prepared from a hydroxide and is of relatively low purity.

(c) BeO designated herein as HPA grade which is from a hydroxide of relatively high purity (derived from the beryllium basic acetate process(1)) and mostly supplied by the Mineral Concentrates Company.

The UOX and HPA grades were modified by adding 0.5 weight percent MgO as a sintering aid(2) and the UOX grade was also modified by the use of 3 weight percent ZrO_2 to restrict grain growth(3). An organic material was added to two of the "compositions" where it was desirable to have both high porosity and large grain sizes in the same sample.

BeO Powders

The BeO powders were characterized by determining the chemical analysis, specific surface area, particle size and distribution, crystallite size, and examination by both optical and electron microscopy.

Impurity Content - The impurity content of the three types of BeO powders are shown in Table I for the lots of each type used in this study. From these data it is seen that the AOX grade is the less pure with respect to non-volatile impurities, showing considerably more lithium, magnesium, manganese, sodium, silicon, strontium and zinc than the other two types.

Specific Surface Area and Crystallite Size - The specific surface area of each lot of BeO was measured by the BET method. The crystallite sizes were measured by X-ray diffraction line broadening techniques. The data for both of these characteristics are listed in Table II along with the calculated particle size based on the specific surface area. According to these data, the AOX grade material is of the smallest particle size.

Particle Size and Distribution - The results of Coulter Counter analyses of the three grades of BeO are shown in

TABLE I

CHEMICAL ANALYSES OF BeO POWDERS

	UOX Grade			AOX Grade		
Element	Lot 200-W-89	Lot 200-W-111	Lot 200-W-162	Lot 6	Lot 7	Lot 10
C	170 ppm	110 ppm	90 ppm	- **	350 ppm	290 ppm
F	N*<10	N*<10	N*<10	- **	13	320
P	9	10	N*<10	- **	28	N*
S	400	430	580	<50	54	9
Al	35	30	20	<1	20	10
Ag	N*<5	N*<5	N*<5	- **	- **	N*<3
B	N*<3	N*<3	N*<3	<1	N*<3	N*<3
Ba	N*<10	N*<10	N*<10	10	- **	N*<10
Ca	N*<10	100	N*<10	65	30	40
Cd	N*<10	N*<10	N*<10	<1	- **	N*<3
Co	N*<5	N*<5	N*<5	<1	- **	N*<3
Cr	N*<10	N*<10	N*<10	19	10	20
Cu	N*<5	N*<5	N*<5	6	- **	N*<3
Fe	15	15	30	6	10	40
Li	N*<1	1	N*<1	100	40	50
Mg	15	20	30	135	250	90
Mn	N*<10	N*<10	N*<10	285	90	100
Mo	N*<10	N*<10	N*<10	- **	- **	N*<10
Na	N*<5	20	20	200	1000	500
Ni	N*<10	N*<10	N*<10	7	N*<10	N*<10
Pb	N*<10	N*<10	N*<10	- **	- **	N*<10
Si	35	25	15	230	475	300
Sn	N*<10	N*<10	N*<10	- **	- **	N*<10
Sr	N*<10	N*<10	N*<10	30	- **	60
Ti	N*<10	N*<10	N*<10	- **	- **	N*<10
Zn	N*<20	N*<20	N*<20	- **	- **	60
L.O.D.(d) @ 110°C	0.07%	0.23%	0.21%	0.30%	0.24%	N*
L.O.I.(e) @ 1350°C	0.25%	0.41%	0.21%	0.34% (1000°C)	0.46%	0.20%

* N means not detected and the number following signifies the detection limit.

** - means not analyzed.

TABLE I (Continued)

	HPA Grade					
Element	Lots K-96 & K-121(a)	Lot K-111(a)	Lot K-123(a)	Lot 1350(b)	Lot 144(c)	Lot 146-R(c)
C	- **	- **	- **	158 ppm	210 ppm	- **
F	N*<10 ppm	15 ppm	10 ppm	N*<10	N*<5	- **
P	19	N*<10	21	12	N*	- **
S	13	37	35	15	140	- **
Al	15	25	30	25	70	30
Ag	- **	- **	- **	N*<5	N*<5	N*<5
B	N*<3	N*<3	N*<3	N*<3	N*<3	N*<3
Ba	- **	- **	- **	N*<10	N*<10	N*<10
Ca	N*<10	- **	- **	50	N*<10	N*<10
Cd	- **	- **	- **	N*<3	N*<3	N*<3
Co	- **	N*<5	N*<5	N*<5	N*<10	N*<10
Cr	N*<5	N*<10	N*<10	N*<10	N*<10	N*<10
Cu	- **	- **	- **	N*<5	N*<5	N*<5
Fe	15	20	35	30	60	15
Li	- **	- **	- **	N*<1	N*<1	N*<1
Mg	N*<10	N*<10	N*<10	50	N*<10	N*<10
Mn	- **	- **	- **	N*<10	N*<10	N*<10
Mo	N*<10	- **	- **	N*<10	N*<10	N*<10
Na	N*<10	N*<10	N*<10	40	N*<10	N*<10
Ni	- **	- **	- **	N*<10	N*<10	N*<10
Pb	- **	- **	- **	N*<10	N*<10	N*<10
Si	10	20	35	70	170	80
Sn	- **	- **	- **	N*<10	N*<10	N*<10
Sr	- **	- **	- **	N*<10	N*<10	N*<10
Ti	- **	- **	- **	N*<10	N*<10	N*<10
Zn	- **	- **	- **	N*<20	N*<20	N*<20
L.O.D.(d) @ 110°C	- **	- **	- **	0.04%	0.32%	- **
L.O.I.(e) @ 1350°C	- **	- **	- **	0.01%	0.15%	- **

---

a) GE-NMPO lot number.

b) GE-NMPO lot number assigned to Minox AAA BeO powder calcined at 1350°C.

c) Minox AAA lot number.

d) L.O.D. = loss on drying.

e) L.O.I. = loss on ignition.

TABLE II

SURFACE AREAS AND CRYSTALLITE SIZES OF BeO POWDERS

	Specific Surface Area[a] (m^2/g)	Equivalent Diameter[b] (microns)	Crystallite Size[c] (Angstroms)
UOX Grade			
Lot 200-W-89	11.8	0.17	1400
Lot 200-W-111	11.2	0.18	1400
Lot 200-W-162	13.5	0.15	650
AOX Grade			
Lot 6	17.9	0.11	450
Lot 7	19.8	0.10	600
Lot 10	18.7	0.11	500
HPA Grade			
Lot K-111[d]			400
Lot AAA 1350[e]	0.849	2.35	1600
Lot AAA 144[f]	13.2	0.15	550
Lot AAA 145-R[f]	12.2	0.16	575

---

a) As measured by BET method.

b) Calculated diameter of equal-size spheres having measured specific surface.

c) As determined by X-ray diffraction line broadening techniques.

d) GE-NMPO lot number.

e) GE-NMPO lot number assigned to Minox AAA BeO powder calcined at 1350°C.

f) Minox AAA lot number.

Fig. 1. They are discussed below in conjunction with the electron microscopy results.

Electron Microscopy - Electron micrographs of the BeO powders are shown in Figures 2 to 5. It is to be noted that while the 50,000 magnification micrographs show the ultimate particles to be similar in all three grades of powder, the lower magnification micrographs show agglomeration to be more prevalent in the AOX HPA grades than in UOX. This is consistent with the Coulter Counter plots of Fig. 1, which show AOX and HPA to have relatively large fractions of material greater than two microns. These are probably agglomerates of crystallite since the x-ray diffraction and surface area measurements indicate a particle and/or crystallite size of only a fraction of a micron. (See Table II). Evidence of the influence of agglomeration on Coulter Counter plots is contained in the two curves for HPA lot 10 in Fig. 1c, which shows that comminution by a jet pulverizer was effective in reducing the amount of powder larger than two microns.

Light Microscopy - The transmitted polarized light micrographs in Fig. 6 show that many needle-like particles are present in the UOX grade BeO. These needles are considered to be the primary cause of preferred orientation of grains in extruded and sintered UOX grade specimens(4).

Fig. 1 Coulter Counter analyses of (a) UOX grade, (b) AOX grade, and (c) HPA grade BeO powders.

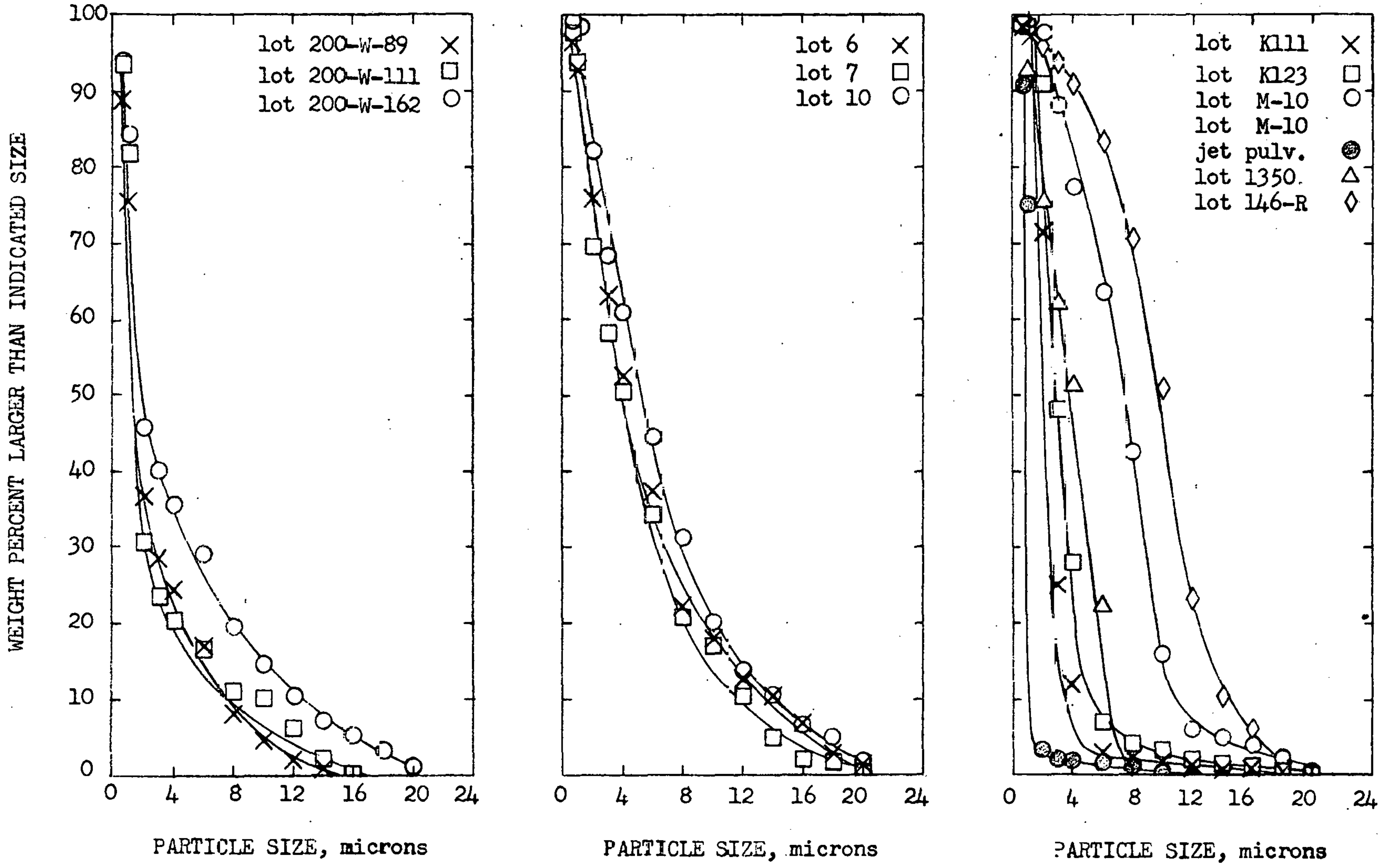

(a)

(b)

(c)

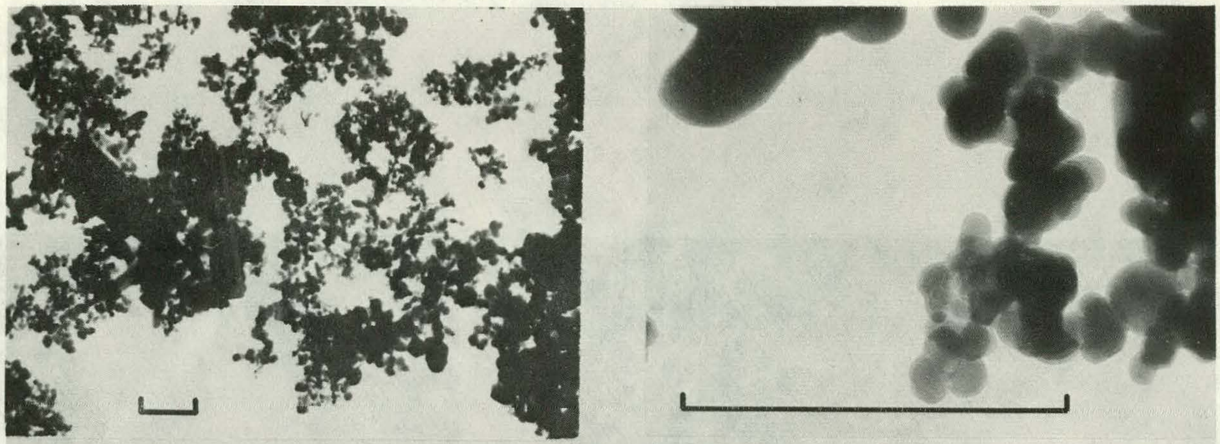

Neg. 628-C (a) 7,500X

Neg. 630-B (b) 50,000X

Fig. 2. Electron micrographs of UOX grade BeO powder, lot 200-W-162. (Reference mark equal 1 micron).

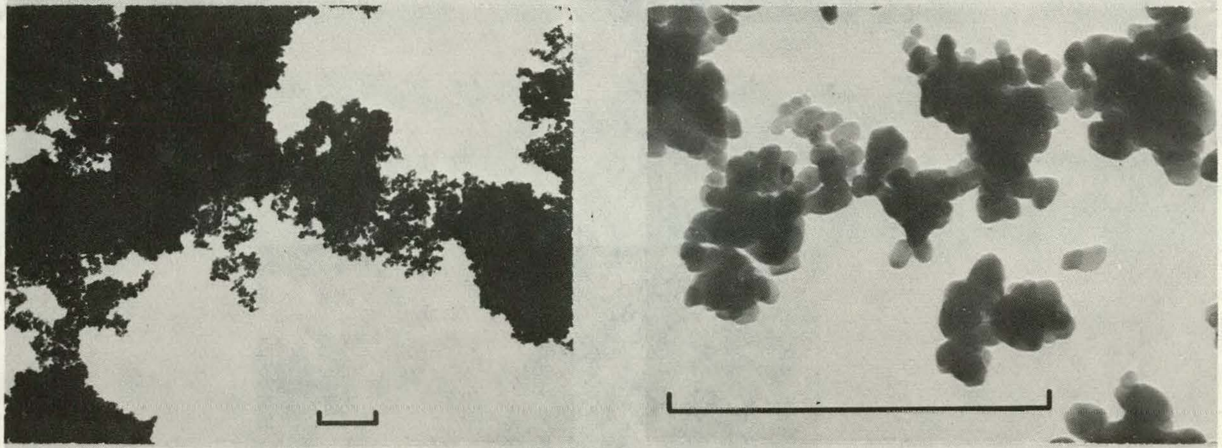

Neg. 631-B (a) 7,500X

Neg. 632-C (b) 50,000X

Lot 6

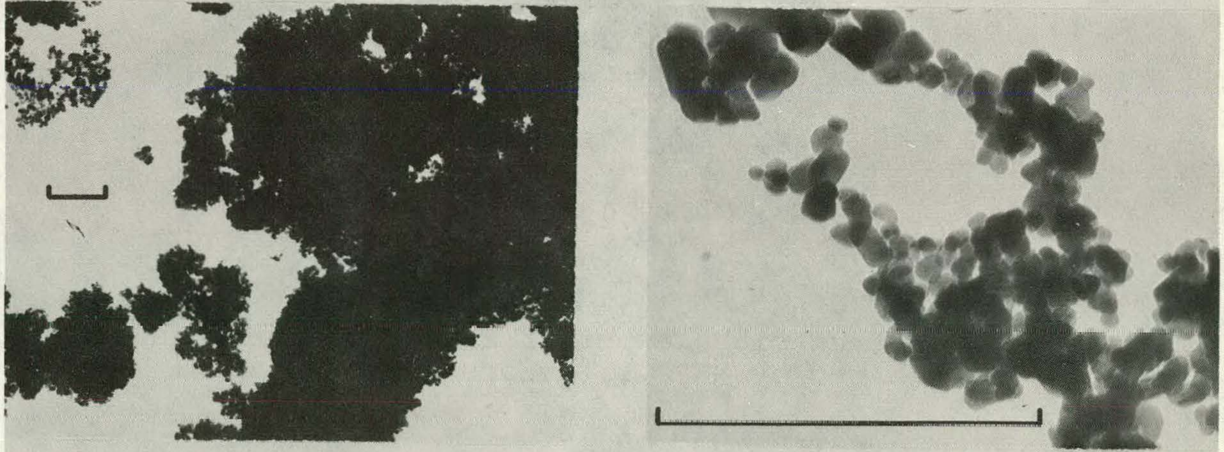

Neg. 633-C (c) 7,500X

Neg. 634-A (d) 50,000X

Lot 7

Fig. 3. Electron micrographs of AOX grade BeO powders. (Reference mark equal 1 micron.)

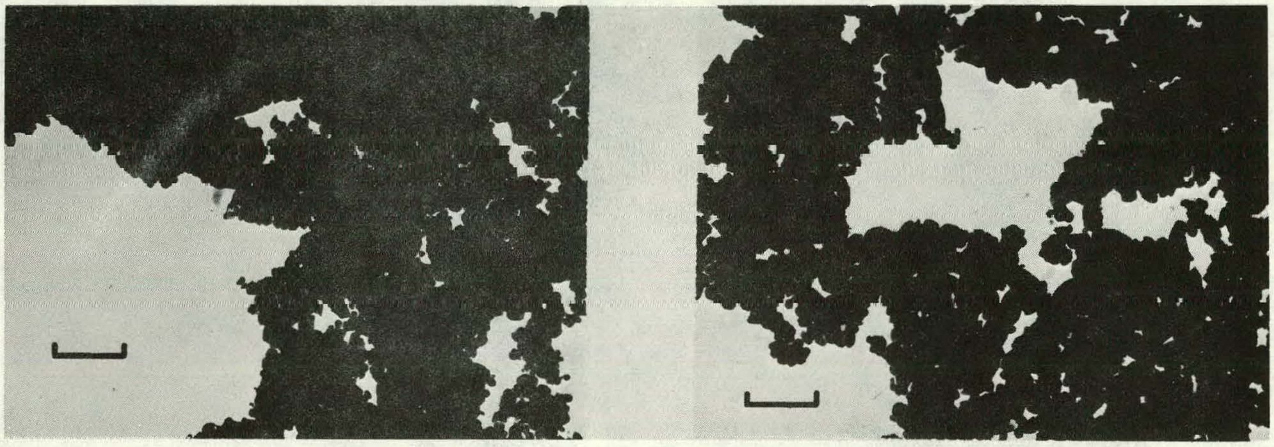

Neg. 452-A (a) 9,100X

Lot M-6, vibratory milled

Neg. 456-C (b) 9,100X

Lot M-7, Jet Pulverized

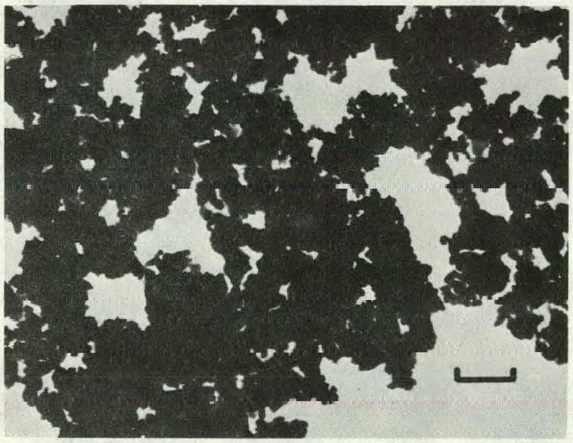

Neg. 454-E (c) 7,500X

Lot M-10, Jet Pulverized

Fig. 4. Electron micrographs of HPA grade BeO: Mincon $Be(OH)_2$ calcined by NMPO. (Reference marks equal 1 micron.)

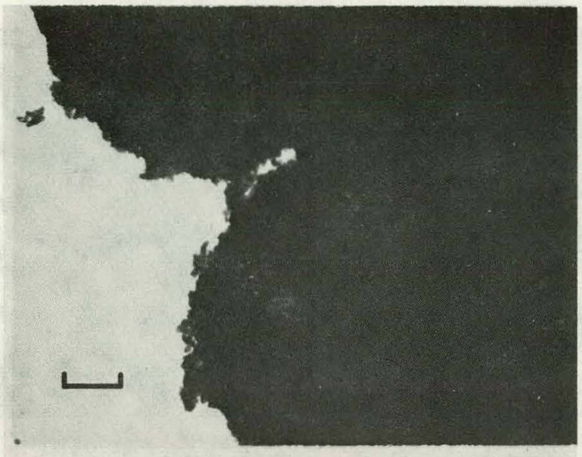

Neg. 644-E 7,500X

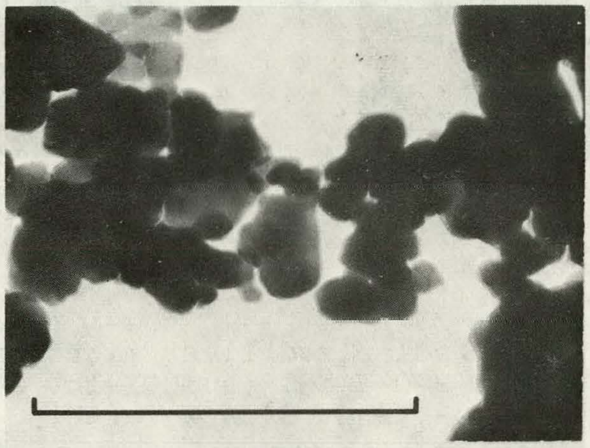

Neg. 645-C 50,000X

lot 146-R

Fig. 5 Electron micrographs of HPA grade BeO: Minox AAA Powders (reference mark equal 1 micron)

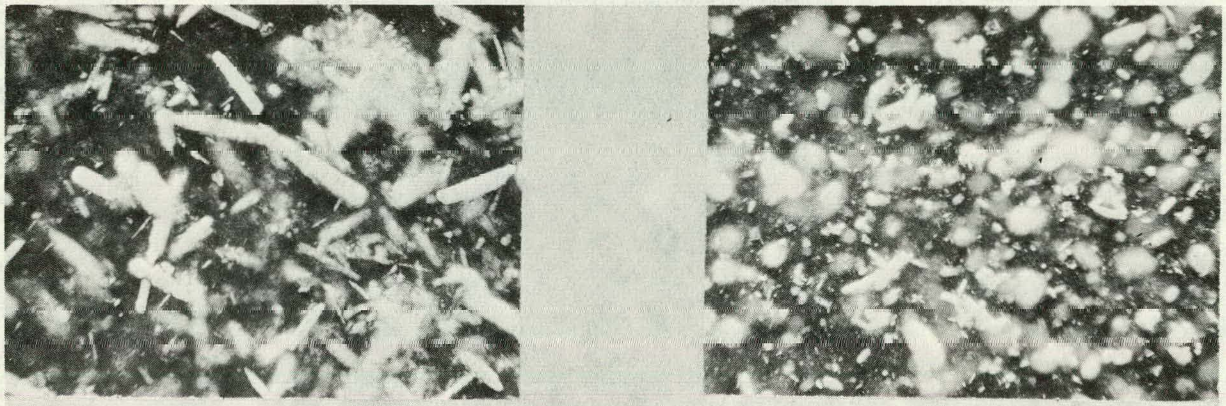

Neg. 1521 (a) 250X

Neg. 1524 (b) 100X

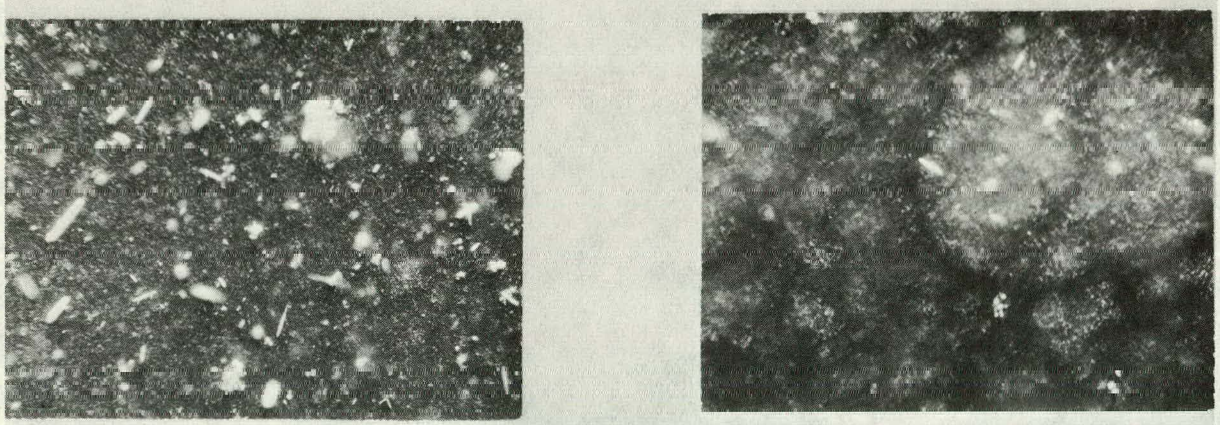

Neg. 1525 (c) 100X

Neg. 1526 (d) 250X

Fig. 6. Transmitted polarized light micrographs of BeO powders: (a) UOX lot 200-W-89, (b) UOX lot 200-W-111, (c) UOX lot 200-W-162, and (d) AOX lot 7.

Additives

MgO Powder - The MgO powder used as a minor addition (0.5 w/o) to some of the compositions was Mallinckrodt's S.L. grade, lot number G1518 NY01. Its impurity content is given in Table III. The supplier's screen analysis shows that 90% of the powder passes through 325 mesh and less than one percent is retained on 100 mesh screen.

ZrO_2 - ZrO_2 was added both as a powder and as a sol. The ZrO_2 powder was Wah Chang Corporation's nuclear grade having a particle size of less than five microns. Its impurity content is given in Table III.

The ZrO_2 sol was supplied by W. R. Grace and Company. It was a nuclear grade water suspension, lot number 1207-35, containing 3.63 w/o ZrO_2 of 3 to 7 millimicron particle size. The impurity content (on ZrO_2 basis) is also given in Table III. Other available information on this sol are that the density is 1.036 g/cm^3, the pH is 2.8, the relative viscosity is 1.94, and the specific conductance is 6.21×10^{-2} mho/cm.

Phenolic Resin - The ranges of densities and grain sizes needed for the task were too broad to be obtained by sintering time and temperature variations alone. It was also

TABLE III

IMPURITY CONTENTS OF ADDITIVES

		ZrO$_2$		
	MgO(a)	powder(b)	sol(c)	Phenolic Resin(d)
C	1000 ppm	77 ppm		
Cl	40		20 ppm	
F	40		188	
N	N*<10		6.8%	
P	30		15 ppm	
S	10	30	N*<54	
Ag	10	N*<5	N*<5	N*<100 ppm
Al	30	N*<10	15	500 to 3600
B	N*<1	N*<0.5	20	N*<1000
Ba	N*<10		10	N*<100
Be	50			
Ca	300	10	99	500 to 3600
Cd	N*<3	N*<0.5	N*<9	N*<100
Co	N*<5	N*<10		N*<100
Cr	10	N*<10		50 to 500
Cu	N*<5	N*<5	10	P<100
Fe	30	10	49	P<100
Hf		100	N*<99	
Li	3	N*<1	N*<5	P<100
Mg		N*<10	20	P<100
Mn	N*<10	N*<10	N*<5	N*<100
Mo	N*<10	N*<10	N*<9	P<100
Na	500	30	1477	50 to 500
Ni	10	N*<10	N*<9	P<100
Pb	N*<10	N*<10	15	
Si	100	10	395	500 to 3600
Sn	N*<10	N*<10	9	N*<100
Sr	N*<10			P<100
Ti	N*<10	N*<10	9	50 to 500
Zn		N*<20	N*<20	50 to 500
Zr	20			

---

a) Mallinckrodt S.L. grade, lot G1518 NY01.

b) Wah Chang reactor grade, ANPG 311749.

c) W.R. Grace and Company, lot number 1207-35; values listed based on ZrO$_2$.

d) General Electric Company, number GE-12368.

*N means not detected and the number following signifies the detection limit.

necessary to vary the initial porosity of the samples, and this was done by adding to the BeO an organic "filler" which burned out during the prefiring operation.

Several organic materials were evaluated for this use, and GE-12368 solid phenolic resin was selected on the basis of its particle size (10-50 microns) and the pore size it produced in the resulting microstructure (5-10 microns). The ash content at 1000°C is 0.36 percent and the impurity analysis is given in Table III.

SAMPLE PREPARATION

For the most part, samples were formed by extrusion, although for comparison purposes, a relatively small number of samples were formed by isostatic pressing. The fabrication procedures employed have been described previously$^{(5)}$, but will be briefly summarized here.

Extrusion

The BeO powder was prepared for extrusion by adding a 10.7 w/o aqueous solution of Penford Gum #300, a hydroxyethyl ether derivative of starch, and mixing in a Simpson Muller mixer. Since a small amount of H_2O was lost during mixing, the composition of the mix (for UOX grade BeO) as it was extruded averaged 69.6 w/o BeO, 3.8 w/o Penford Gum, and 26.6 w/o water. When additives were used, they were mixed with the plasticizer prior to mixing with the BeO. The mix was deaired and then extruded at about 6,000 psi head pressure using a hydraulic extrusion press to form 0.352 inch diameter rods. The extruded rods were dried under controlled humidity conditions to prevent warping, then cut to approximately 5.25 inches in length.

Isostatic Pressing

Rods of UOX, and UOX + 0.5 w/o MgO were fabricated by isostatic pressing in order to prepare UOX type samples with random orientation. BeO powder was dispersed in water containing Mobilcer R wax emulsion to give 5 percent binder (on a dry weight basis), dried, and crushed to minus 20 mesh. The material was then prepressed isostatically at 4,000 psi, recrushed to minus 50 mesh, then isostatically pressed at 15,000 psi in rubber molds to form 0.35 inch diameter rods.

Prefiring

All samples were given a prefiring in air at about 800°C to remove the organic matter prior to sintering in hydrogen. Samples were stored at 110°C until sintered to prevent absorption of moisture.

SINTERING OF SAMPLES

Sintering was done in molybdenum box furnaces in an atmosphere of hydrogen. The samples were placed in molybdenum boats as shown in Figure 7. Molybdenum pins were placed between the BeO rods as shown to reduce the probability of warping.

The boats and samples were slowly introduced into the sintering furnace which was at a temperature of about 800°C. The furnace temperature then was raised to the desired sintering temperature at the rate of 200 to 250°C per hour. After sintering, the furnace was allowed to cool to 800°C, and the samples were removed to the furnace cooling chamber.

Approximately 25 cubic feet of dry (-45°C dew point) hydrogen per hour passed through the 1.5 cubic foot hot zone of the furnace.

Sintering conditions varied from 1 to over 100 hours at temperatures of 1340°C to 1700°C. Typical sintering conditions used to obtain the density and grain size

Fig. 7. Arrangement of BeO rods in molybdenum boats during sintering in hydrogen.

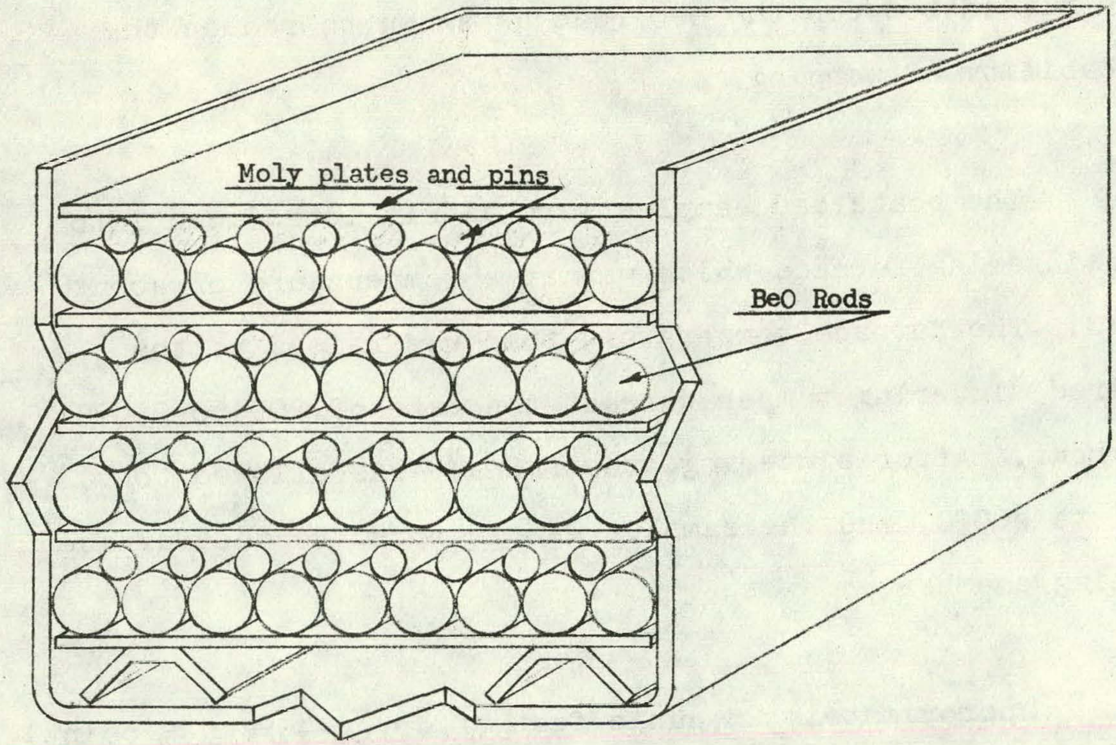

for each composition are given in Table IV. Photomicrographs showing the microstructure of typical samples are shown in Figure 8.

POST-SINTER PROCESSING

The sintered rods, which were about 0.265 inch in diameter, were centerless ground to 0.238 ± .001 inch diameter and cut to 3.500 ± 0.003 inches in length. After they had been cleaned, the rods were inspected for flaws by Zyglo, X-ray, and ultrasonic transmission. They were then heated to 425°C for 1 hour to remove the Zyglo penetrant.

Table V gives the average content of the most abundant impurities in the rods of the three types of BeO after this processing. These data show that there is little difference between samples of the three types after fabrication as far as impurities are concerned. Comparison of the data in Table V with the data in Table I, the impurities present in the starting powders, shows that some impurities such as fluorine, sulfur, lithium, and sodium have decreased in content while others, primarily aluminum, iron, chromium, and nickel have increased slightly.

Fig. 8. Microstructure of Typical sintered samples. (All mag. 250X; 50% HF etchant; density (g/cm3) and grain size (micron) follow Neg. No.

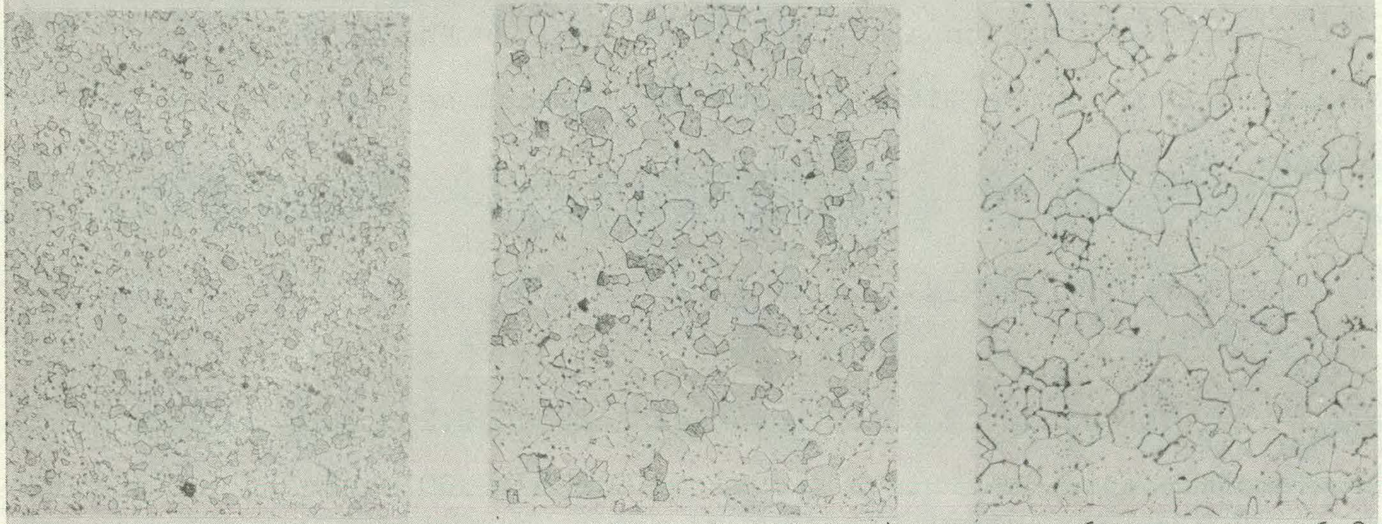

Neg. 1133 - 2.903 - 5

Neg. 1129 - 2.933-10.4

Neg. 699- 2.919-16.8

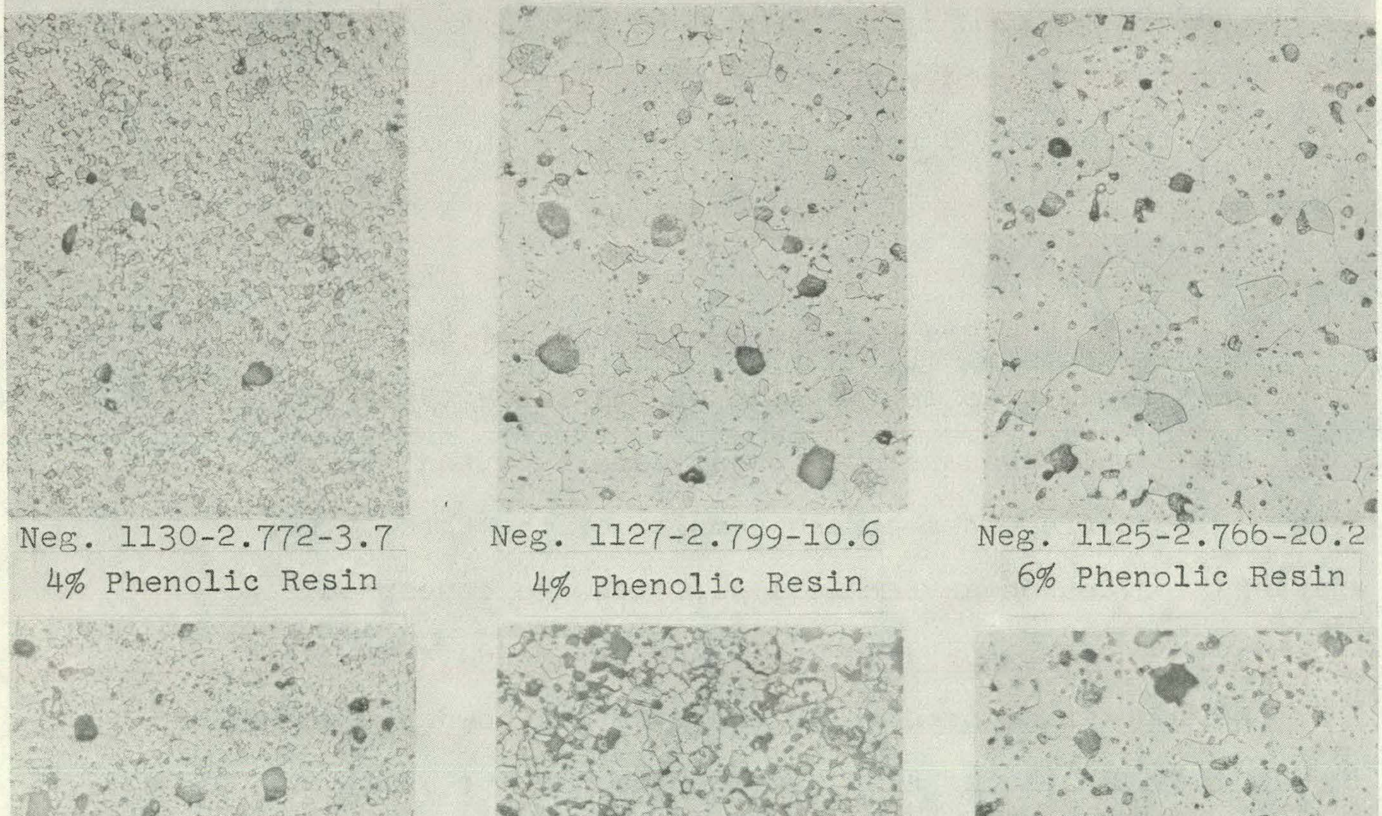

Neg. 1130-2.772-3.7

4% Phenolic Resin

Neg. 1127-2.799-10.6

4% Phenolic Resin

Neg. 1125-2.766-20.2

6% Phenolic Resin

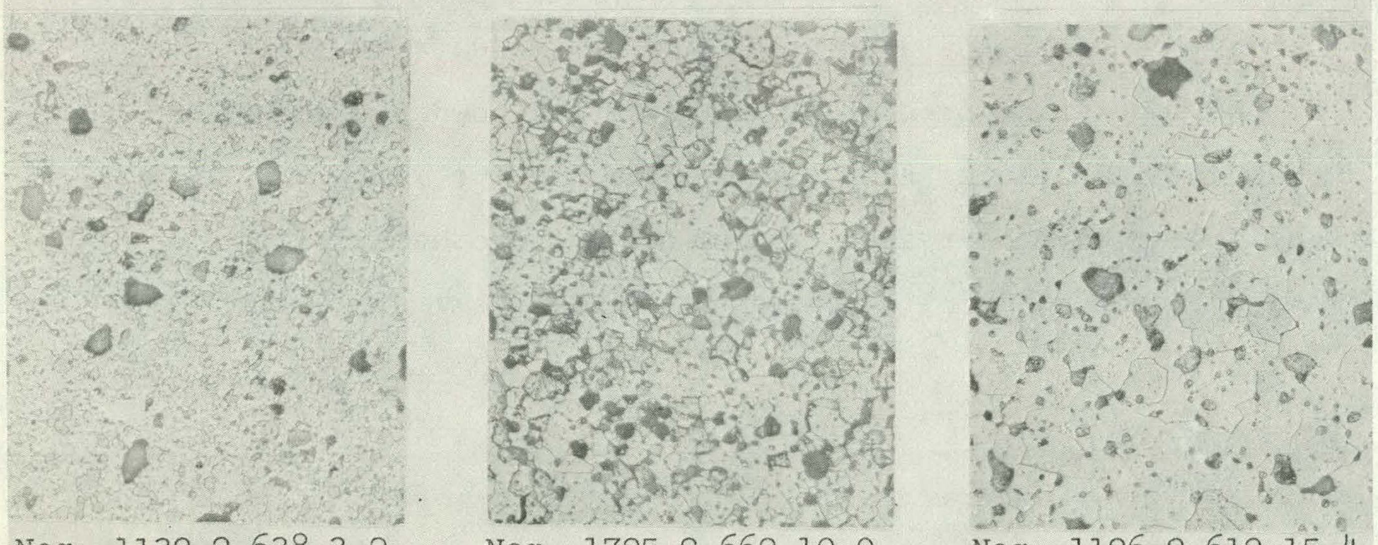

Neg. 1132-2.638-3.9

10% Phenolic Resin

Neg. 1795-2.669-10.0

10% Phenolic Resin

Neg. 1126-2.612-15.4

12% Phenolic Resin

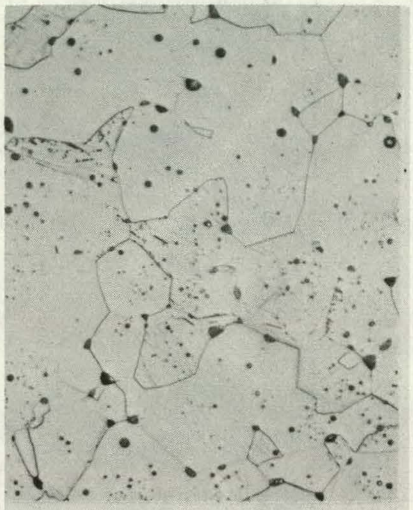

Neg. 817-2.902-45.1

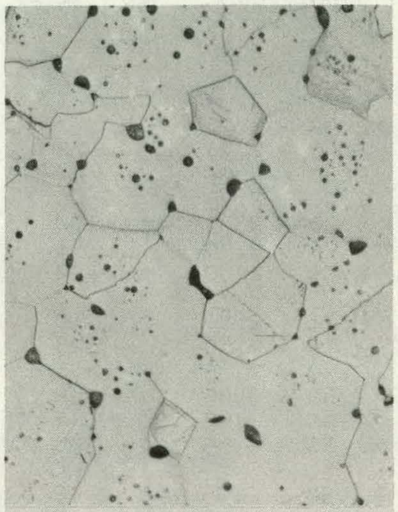

Neg. 818-2.902-68.1

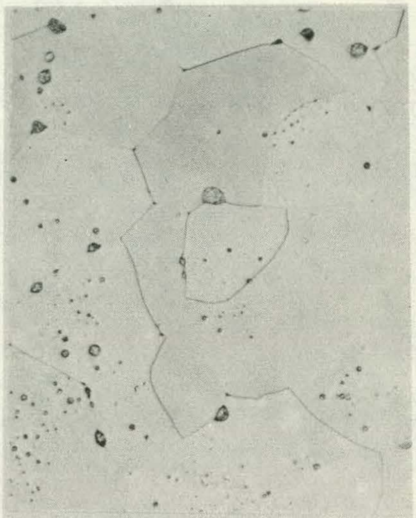

Neg. 1131-2.971-92.9

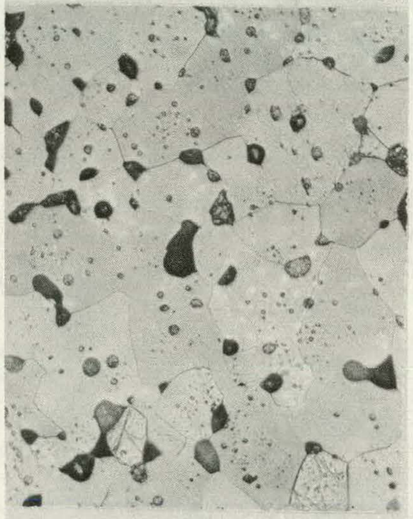

Neg. 1118-2.752-45.7
8% Phenolic Resin

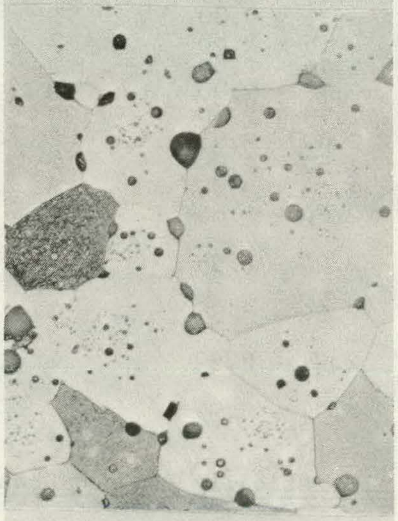

Neg. 1134-2.803-63.0
8% Phenolic Resin

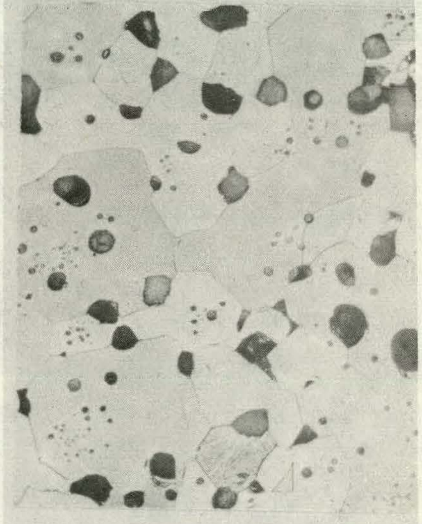

Neg. 1135-2.655-42.6
16% Phenolic Resin

TABLE IV

TYPICAL SINTERING CONDITIONS FOR TARGET DENSITIES AND GRAIN SIZES

Composition	Grain Size Microns	Density g/cm^3	Sintering Conditions in Hydrogen Atmosphere		Phenolic Resin Added Weight Percent
			Time in Hours	Temp. in °C	
HPA	15-20	2.90 - 2.95	4	1700	None
	38-50	2.90 - 2.95	24	1700	"
	60-80	2.90 - 2.95	35	1700	"
	90-120	2.90 - 2.95	64	1700	"
	<5	2.75 - 2.80	1	1670	"
UOX + 0.5 w/o MgO	<5	2.90 - 2.95	1	1430	"
	9-12	2.90 - 2.95	2	1445	"
	15-20	2.90 - 2.95	2	1510	"
	38-50	2.90 - 2.95	24	1700	"
	60-80	2.90 - 2.95	60	1700	"
	90-120	2.90 - 2.95	100	1700	"
	<5	2.75 - 2.80	1	1400	4
	9-12	2.75 - 2.80	2	1425	4
	15-20	2.75 - 2.80	2	1530	6
	38-50	2.75 - 2.80	10	1700	8
	60-80	2.75 - 2.80	125	1700	8
	<5	2.60 - 2.65	1	1400	10
	9-12	2.60 - 2.65	2	1425	10
	15-20	2.60 - 2.65	2	1560	12
	38-50	2.60 - 2.65	50	1700	16
AOX	9-12	2.90 - 2.95	2	1460	None
	15-20	2.90 - 2.95	3	1570	"
	38-50	2.90 - 2.95	24	1700	"
	60-80	2.90 - 2.95	60	1700	"
	90-120	2.90 - 2.95	120	1700	"
	<5	2.75 - 2.80	1	1490	2
	9-12	2.75 - 2.80	2	1575	(a)
	15-20	2.75 - 2.80	3	1600	4
	38-50	2.75 - 2.80	20	1700	8
	60-80	2.75 - 2.80	120	1700	8
	<5	2.60 - 2.65	2	1430	8
	9-12	2.60 - 2.65	2	1530	8
	15-20	2.60 - 2.65	8	1625	10
	38-50	2.60 - 2.65	40	1700	16
HPA + 0.5 w/o MgO	15-20	2.90 - 2.95	2	1540	None
UOX	15-20	2.90 - 2.95	1	1700	"
UOX + 3 w/o ZrO_2	15-20	2.94 - 2.99	1	1700	"
UOX + 3 w/o ZrO_2 sol	15-20	2.94 - 2.99	2	1700	"
		Isostatically Pressed Rods			
UOX + 0.5 w/o MgO	15-20	2.90 - 2.95	2	1550	"
AOX	15-20	2.90 - 2.95	3	1570	"
UOX	15-20	2.90 - 2.95	2	1700	"
		One-Inch Diameter Specimens			
UOX + 0.5 w/o MgO	15-20	2.90 - 2.95	2	1640	"
AOX	15-20	2.90 - 2.95	2	1700	"
UOX	15-20	2.90 - 2.95	2	1700	"
UOX + 3 w/o ZrO_2	15-20	2.90 - 2.95	2	1700	"

---

a) Batch contained 50 w/o AOX powder calcined for 2 hours at 1290°C.

TABLE V

MOST ABUNDANT IMPURITIES IN SINTERED BeO SAMPLES

	UOX[(a)]	AOX[(b)]	HPA[(c)]
C	133	139	192
F	12	N<10[(d)]	17
P	24	13	24
S	49	23	27
Al	132	50	76
Ba	22	24	32
Ca	95	65	22
Cr	15	9	27
Fe	113	73	164
Li	1	5	N<1
Mg	80	125	41
Mn	N<10	35	N<10
Na	12	11	12
Ni	23	28	26
Si	110	303	123
Sr	N<10	45	N<10

---

a) Average of 32 samples including some UOX + 0.5 w/o MgO and UOX + 3 w/o ZrO_2 samples; samples with MgO added not included in Mg analyses.

b) Average of 18 samples.

c) Average of 9 samples including some HPA + 0.5 w/o MgO samples; samples with MgO added not included in Mg analyses.

d) N < = not detected; less than (number).

The aluminum may have been introduced during sintering since it has been observed that aluminum content increases slightly with increasing sintering temperatures and times. The iron, chromium, and nickel contaminants were introduced during fabrication.

Part of the MgO added to BeO is lost during sintering in hydrogen, apparently by volatilization(6). The amount lost is dependent on the time, temperature and porosity as shown by the data in Table VI.

RESULTS AND DISCUSSION

The two major occurrences during sintering are densification (shrinkage) and grain growth. While growth of grains is not a requisite of the sintering process, it usually occurs simultaneously, particularly during the sintering of very fine particles such as those used in this work. The densification and grain growth characteristics of the BeO types are described, including the effects of MgO and ZrO_2 additions to the BeO, and the effect of porosity produced by adding a resin which burned out during prefiring.

TABLE VI

MAGNESIA CONTENTS OF BeO - 0.5 w/o MgO RODS SINTERED IN HYDROGEN

Sintered Density (g/cm^3)	MgO Content (%)	Sintering		Resin Content (w/o)
		Temp. (°C)	Time (Hrs.)	
2.97	0.23	1700	100	0
2.95	0.17	1700	161	0
2.91	0.14	1700	118	0
2.76	0.02	1700	140	8
2.74	0.04	1700	15	8
2.66	0.008	1700	50	16
2.64	0.002	1700	64	16
2.95	0.44	1540	1.75	0
2.92	0.45	1540	1.5	0
2.63	0.38	1540	3.5	12
2.62	0.38	1540	2	12
2.95	0.44	1480	2.5	0
2.78	0.45	1480	2	6
2.75	0.30	1480	2	6
2.61	0.28	1480	2	12

Densification - The sintered densities of samples made from AOX grade BeO and UOX grade BeO + 0.5 w/o MgO are plotted as a function of the logarithm of time of sintering at 1700°C in Figures 9, 10, and 11. An approximate time correction has been made to times less than 20 hours to compensate for the densification that occurred during the heating cycle since these are not strictly isothermal data. The correction was based on the assumption that the rates of sintering(7) (and grain growth(8)) are proportional to exp(-Q/RT), where Q is the activation energy, for these two processes, R is the gas constant, and T is the absolute temperature. Assuming an activation energy of 150 kcal/mole for BeO and 100 kcal/mole for BeO + 0.5 w/o MgO(2b), approximate corrections of 2/3 hour and 1 hour, respectively, were obtained.

The data include samples which contained various quantities of phenolic resin added to lower the sintered density. The steeper slopes of the curves for samples which contained 12 and 16 w/o resin are probably a result of their lower densities, since during the course of sintering the densification rate does decrease as theoretical density is approached. The pores in these samples probably affect the densification rate also, since the size of the artificially induced pores (about 10 - 20 microns)

Fig. 9. Density of AOX grade BeO rods as a function of sintering time at 1700°C in hydrogen. (Times under 20 hours corrected for heating and cooling by adding 2/3 hour.)

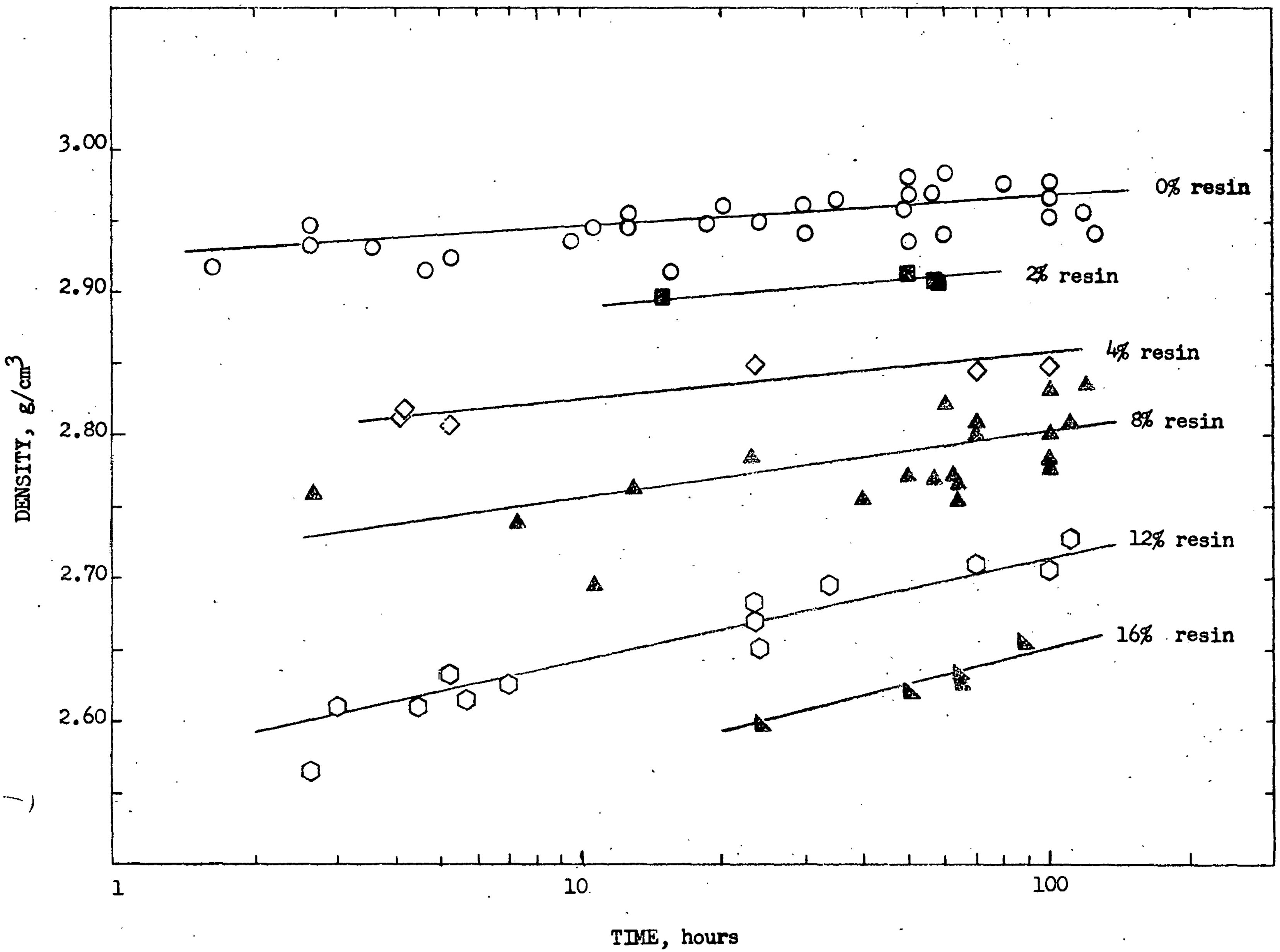

Fig. 10. Density of UOX grade BeO + 0.5 w/o MgO rods as a function of sintering time at 1700°C in hydrogen.

(Times under 20 hours corrected for heating and cooling by adding 1 hour.)

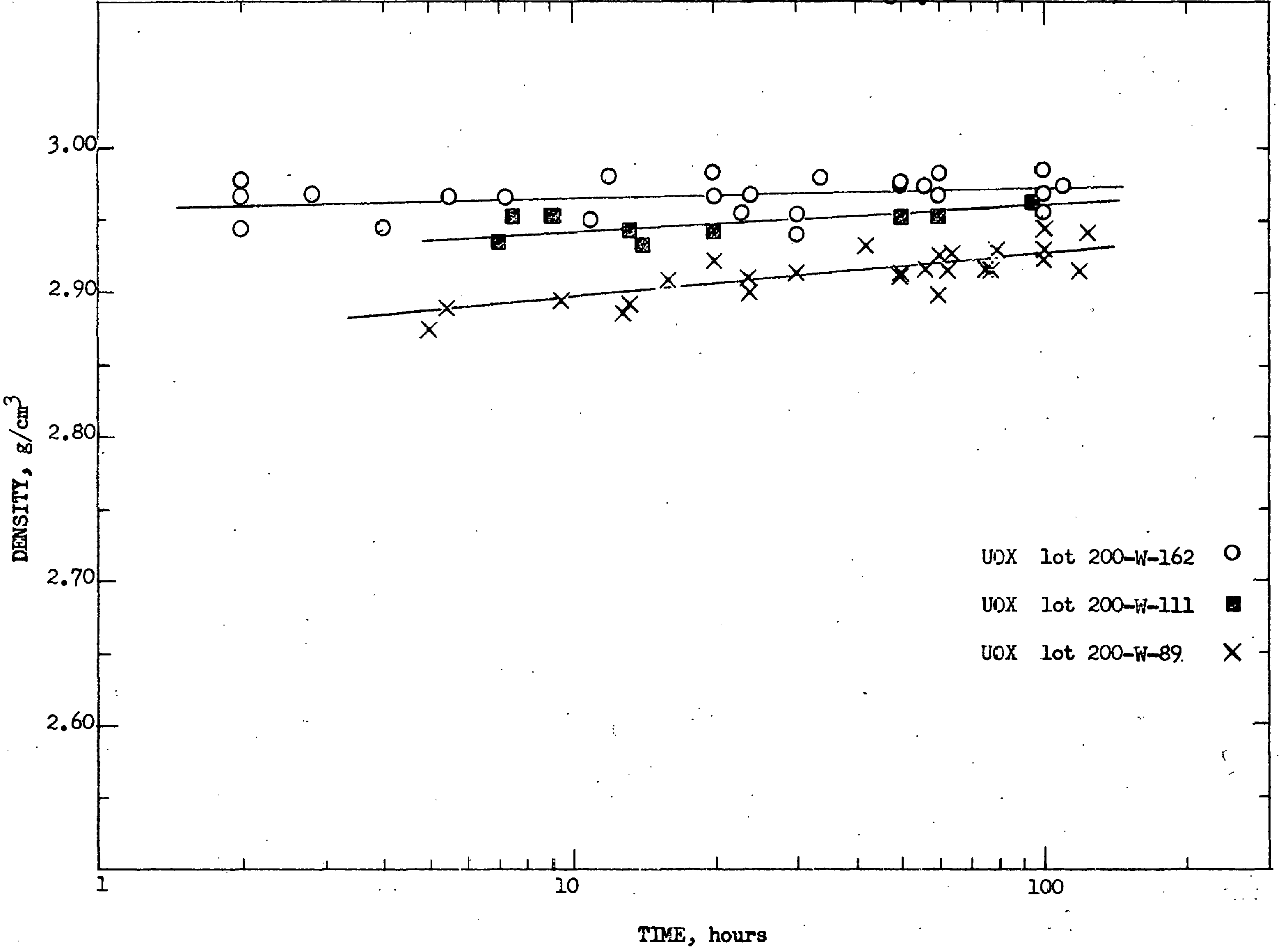

Fig. 11. Density of UOX grade BeO + 0.5 w/o MgO rods made from lot 200-W-162 as a function of sintering time at 1700°C in hydrogen.

(Times under 20 hours corrected for heating and cooling by adding 1 hour.)

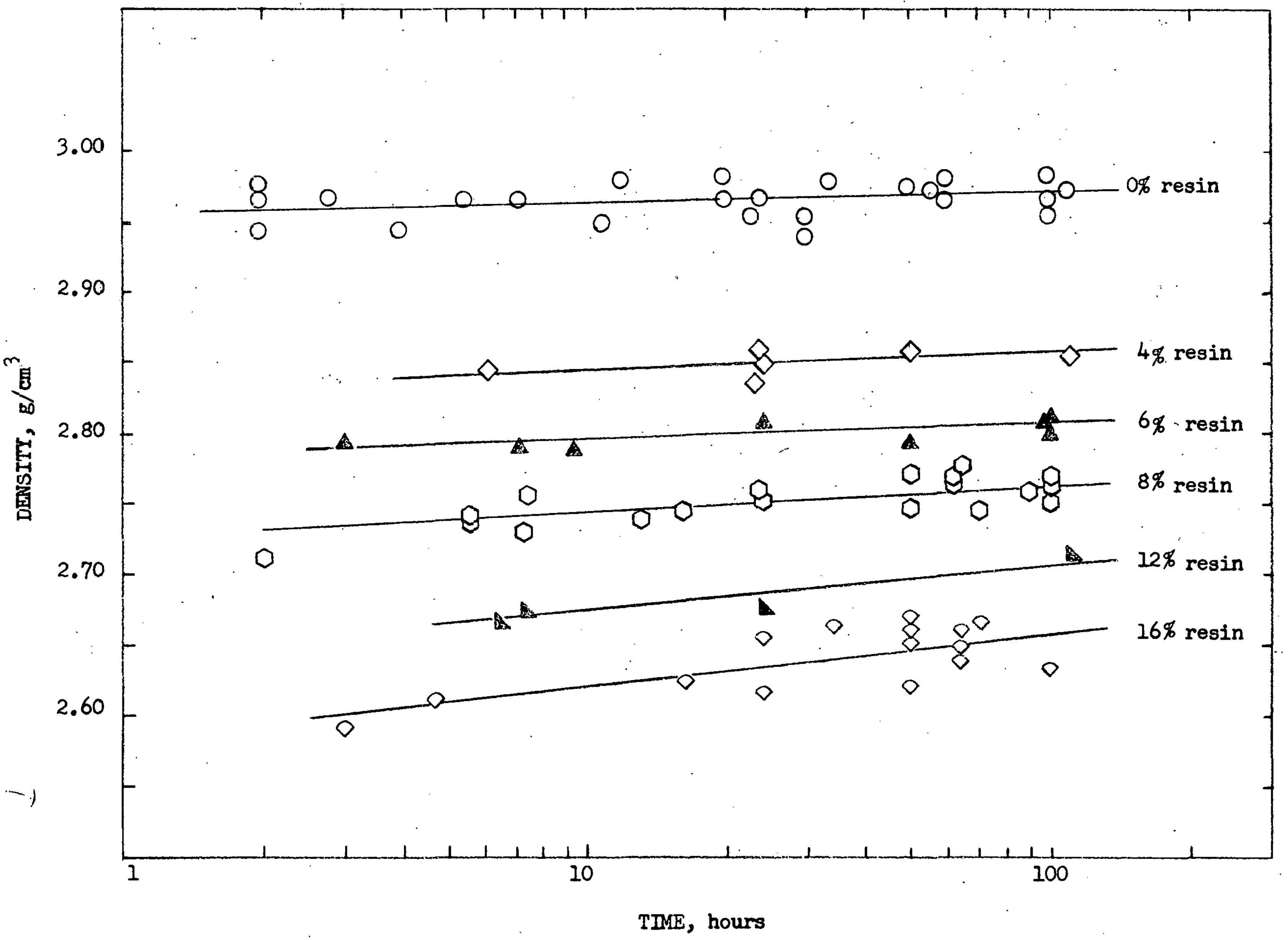

is larger than normally present in the compacted BeO powders of the types used in this study.

Figure 10 contains curves for UOX grade BeO + 0.5 w/o MgO without resin additives. Three lots of the UOX grade powder were used, and three separate curves can be drawn through the data points. The slopes of these curves are slightly different, although this may only be scatter in data. The average green densities of the samples plotted in Figure 10 were 1.437 g/cm^3 for specimens from lot 200-W-162, 1.489 g/cm^3 for lot 200-W-111, and 1.392 g/cm^3 for lot 200-W-89. Therefore, the differences in green density are not the primary cause of the sintered density differences. Coulter Counter and surface area analyses of these powders do not indicate that they are significantly different with respect to average particle size, but the X-ray crystallite size measurements show them to be different, with lot 200-W-162 having an average crystallite size of 650Å and lots 200-W-111 and 200-W-89 both having an average size of 1400Å . Photomicrographs of the powders in Figure 6 show that the amount of large needle-like particles increase in the same order that the sintered densities decrease. This suggests that the differences in sintered densities are related to the large needle-like particles, which cause localized shrinkage rate differences leading to the development of large relatively stable pores.

The data for the UOX grade BeO + 0.5 w/o MgO samples which contained phenolic resin are shown in Figure 11.

Isothermal sinterings were made at 1500° and 1700°C on UOX grade BeO samples, both with and without 0.5 w/o MgO and 3 w/o ZrO_2 (powder and sol). All samples were fabricated from the same lot of BeO (200-W-162) and had approximately equal densities after prefiring (47 - 49% of theoretical). The sintered densities are shown in Figure 12 as a function of the logarithm of time of sintering. These data show that all compositions reached densities in excess of 97% of theoretical in the first hour of sintering at 1700°C, and continue to slowly increase in density with time at this temperature. At 1500°C, only the samples containing MgO sintered to 97% of theoretical density in the first hour.

Figure 13 shows the effect of temperature at a constant sintering time of 2 hours on the density of UOX grade BeO samples both with and without MgO and ZrO_2 additions. These data show that the MgO addition accelerates sintering at temperatures below 1500°C. These data also show somewhat less but similar effects of the ZrO_2 addition.

Fig. 12. Effect of additives on densification of UOX grade BeO at 1500°C and 1700°C in hydrogen.

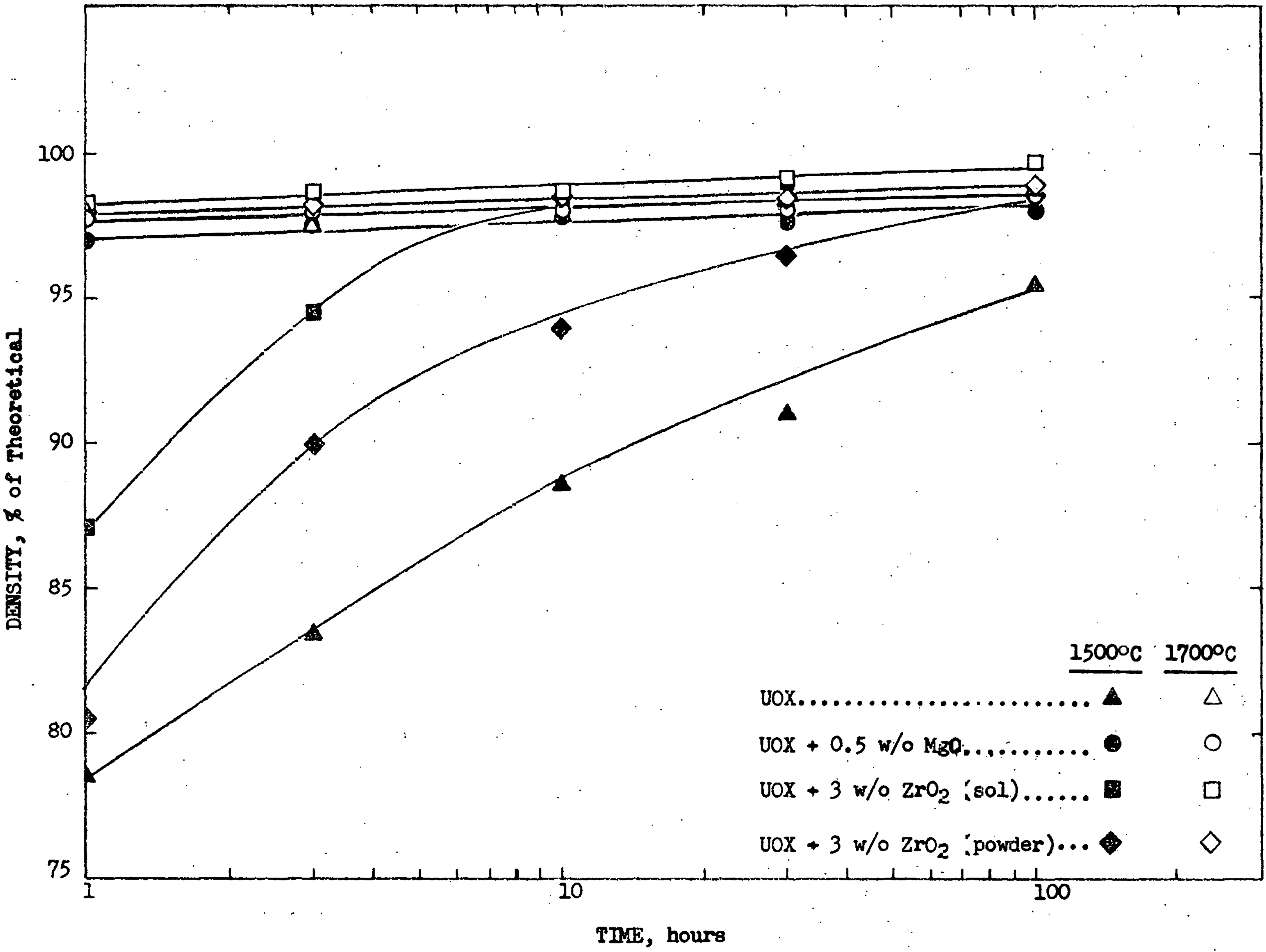

Fig. 13. Effect of additives on density of UOX grade BeO at various sintering temperatures in hydrogen (time constant at 2 hours).

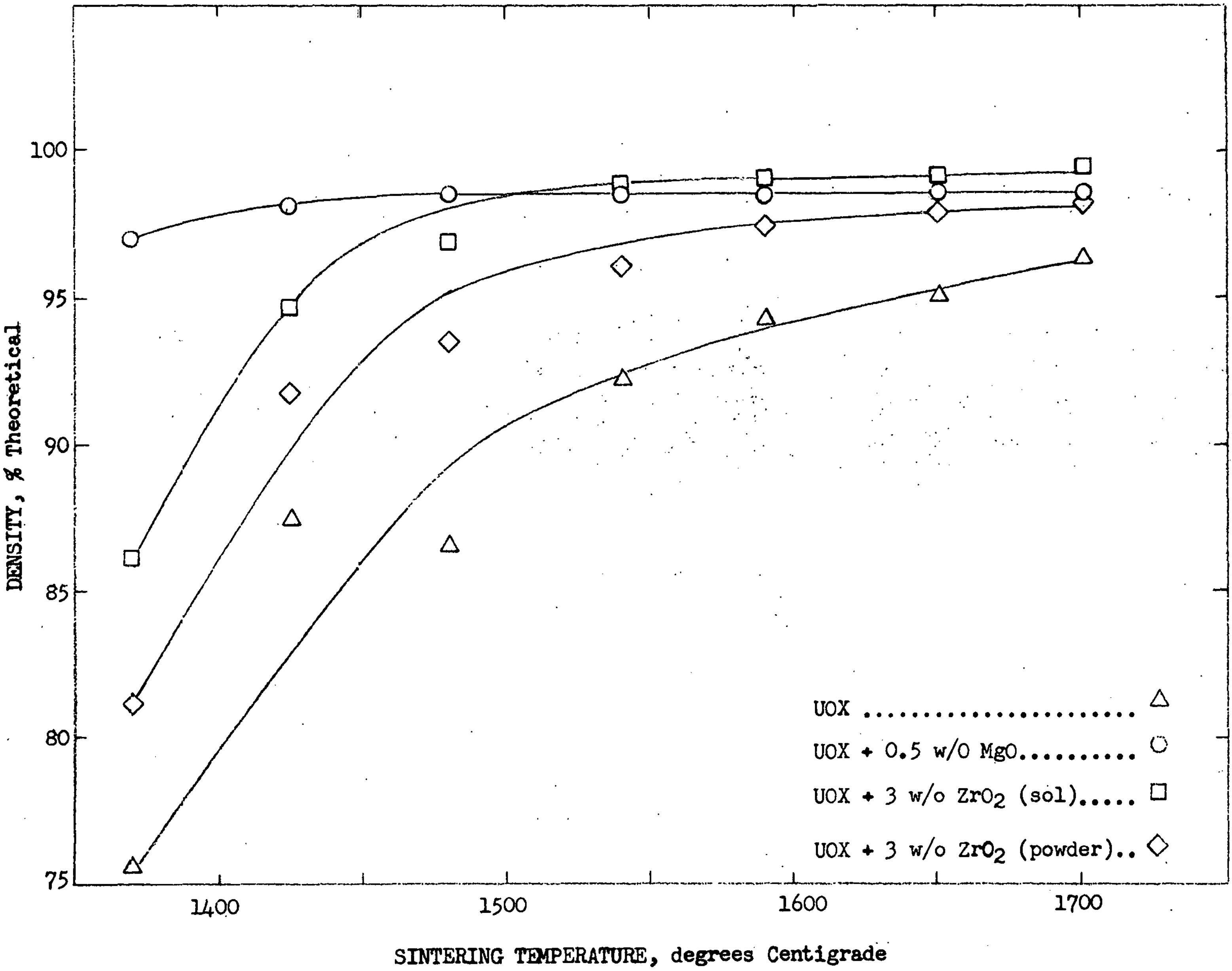

Grain Growth - In a polycrystalline body having grains of uniform size, the grain growth rate is inversely proportional to the size of the grains according to Burke(7), or:

$$\frac{dD}{dt} = \frac{K}{D} \tag{1}$$

where D = instantaneous grain size

and K = temperature-dependent constant

When this equation is integrated to give D as a function of time, the following equation results:

$$D-D_o = K' t^{\frac{1}{2}} \tag{2}$$

where D_o = grain size at t = 0

In practice, the exponent of t has frequently been found to be closer to 1/3 than 1/2 for grain growth in oxides(9). When the initial size of the grain, D_o, is extremely small compared to D, it may be ignored, with the result:

$$D = K' t^{\frac{1}{2}} \tag{3}$$

In Figures 14 through 19, grain size and time are shown in a log.-log. plot in order that the exponent of time in equation (3) can be computed from the slopes of the curves. Here again, the data for times less than 20 hours have been corrected for grain growth which occurred during the heating and cooling cycles by adding 2/3 hour to AOX data and 1 hour to UOX + 0.5 w/o MgO data.

Figure 14 shows the data for AOX grade BeO, both with and without phenolic resin additions, sintered at 1700°C in hydrogen. The curve for 0 w/o resin has a slope of 1/2. The slopes of the curves for the BeO containing phenolic resin decrease with increasing quantities of resin, a result not entirely unexpected, since the presence of pores decreases the rate of grain growth as shown by Burke and Turnbull(10), and porosity increases with resin content.

The data for the three lots of UOX + 0.5 w/o MgO powder are shown in Figure 15. These curves all have a slope of approximately 0.3. The relative position of each curve is the same as in the density versus time and temperature plots (see Figure 12). The lot with the largest portion of large needle-like particles has the smallest sintered grain size, and the lot with the smallest portion has the

Fig. 14. Effect of resin additions on grain size of AOX grade BeO at 1700°C in hydrogen.

(Times under 20 hours corrected for heating and cooling by adding 2/3 hour.)

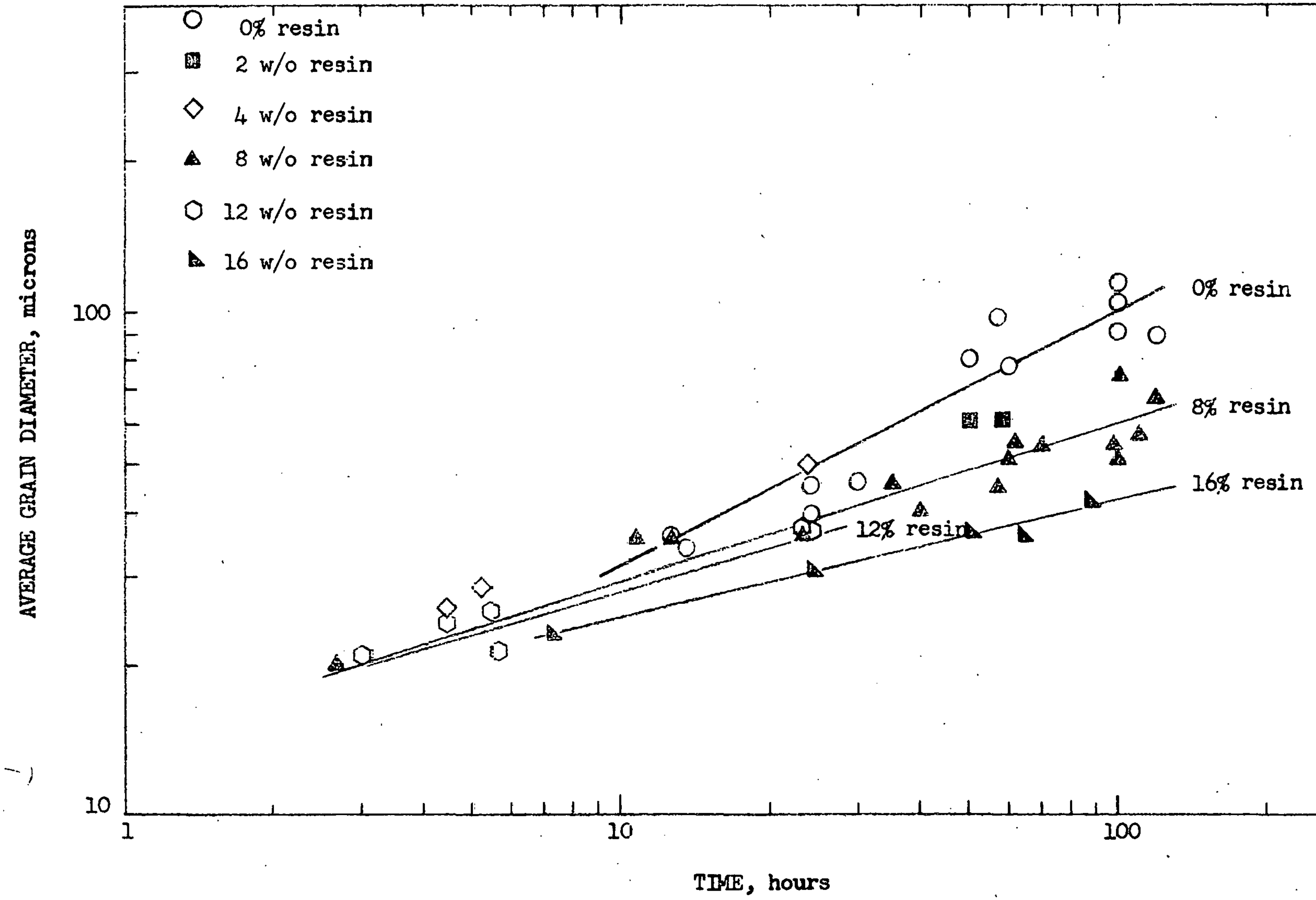

Fig. 15. Grain size of UOX grade BeO + 0.5 w/o MgO rods as a function of sintering time at 1700°C in hydrogen.

(Times under 20 hours corrected for heating and cooling by adding 1 hour.)

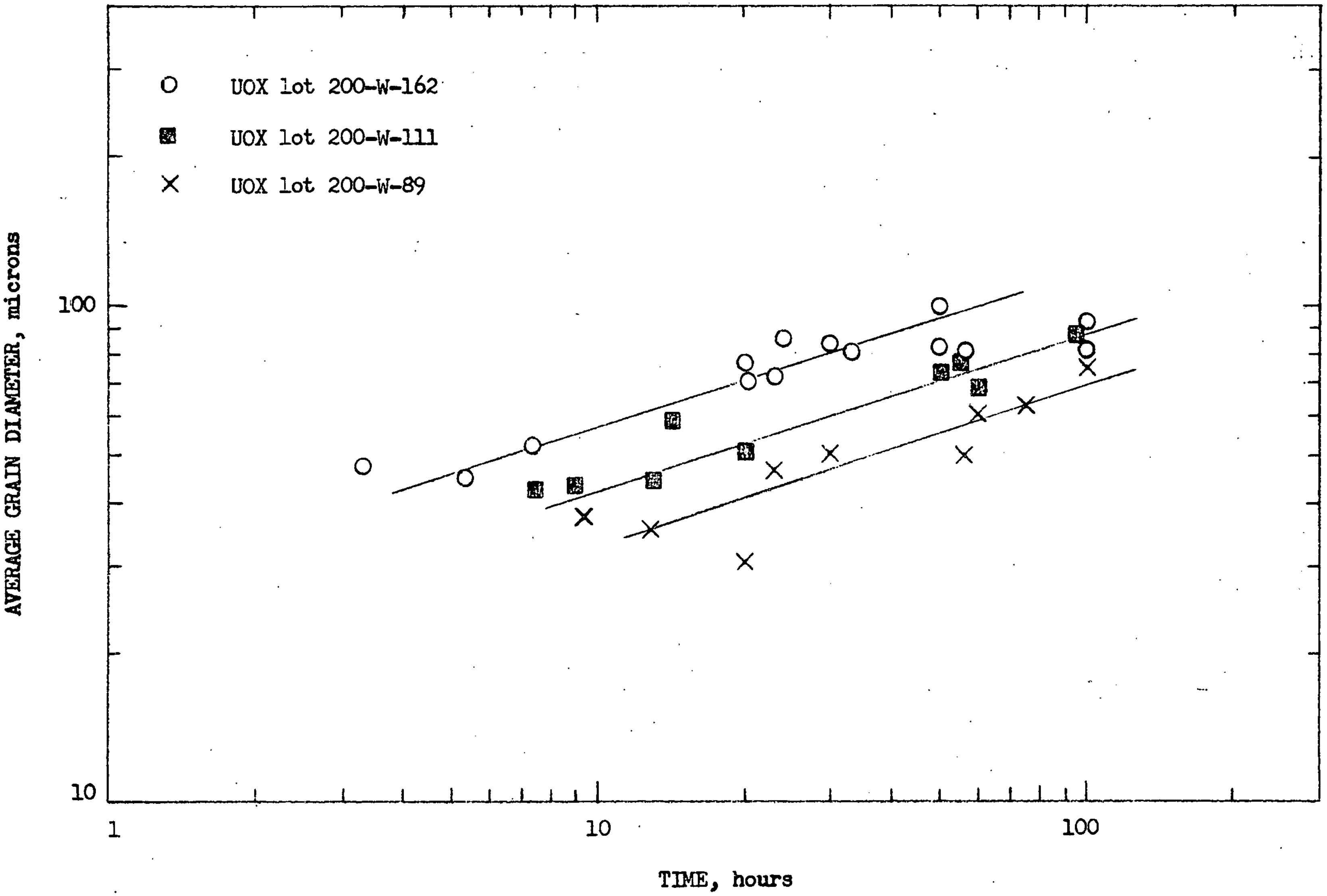

largest sintered grain size. This is qualitatively consistent with Cutler's(11) observations in sintering Al_2O_3, specifically that grain size is an inverse function of the proportion of "nuclei" or large particles present.

Figure 16 shows the effect of phenolic resin additions on the grain size of UOX grade BeO + 0.5 w/o MgO samples sintered at 1700°C in hydrogen. (All of the samples were made from UOX lot 200-W-162.) As with the AOX grade BeO samples, the slopes of the curves decrease as the resin content increases.

Grain size data from the isothermal sinterings of UOX grade BeO samples with and without MgO and ZrO_2 additions at 1500° and 1700°C are given in Figure 17. The slopes of the curves range from about 1/5 to 1/3 for the compositions which attained densities in excess of 95% of theoretical within the first hour at the sintering temperature (see Fig. 12). An exception to this is unadulterated UOX grade BeO sintered at 1700°C. This material showed a steeper initial slope which decreased with time. This would suggest that once the sintering process has reached the point where densification is almost complete, grain growth proceeds at a rate nearly linear with time and that the rate later diminishes to a square root or lower dependence when the average grain size reaches some critical value. One possible explanation of this observation is the occurrence of secondary (discontinuous) grain growth. Although the average size of the grains is smaller than that

Fig. 16. Effect of resin additions on grain size of UOX grade BeO + 0.5 w/o MgO rods made from lot 200-W-162 and sintered at 1700°C in hydrogen.

(Times under 20 hours corrected for heating and cooling by adding 1 hour.)

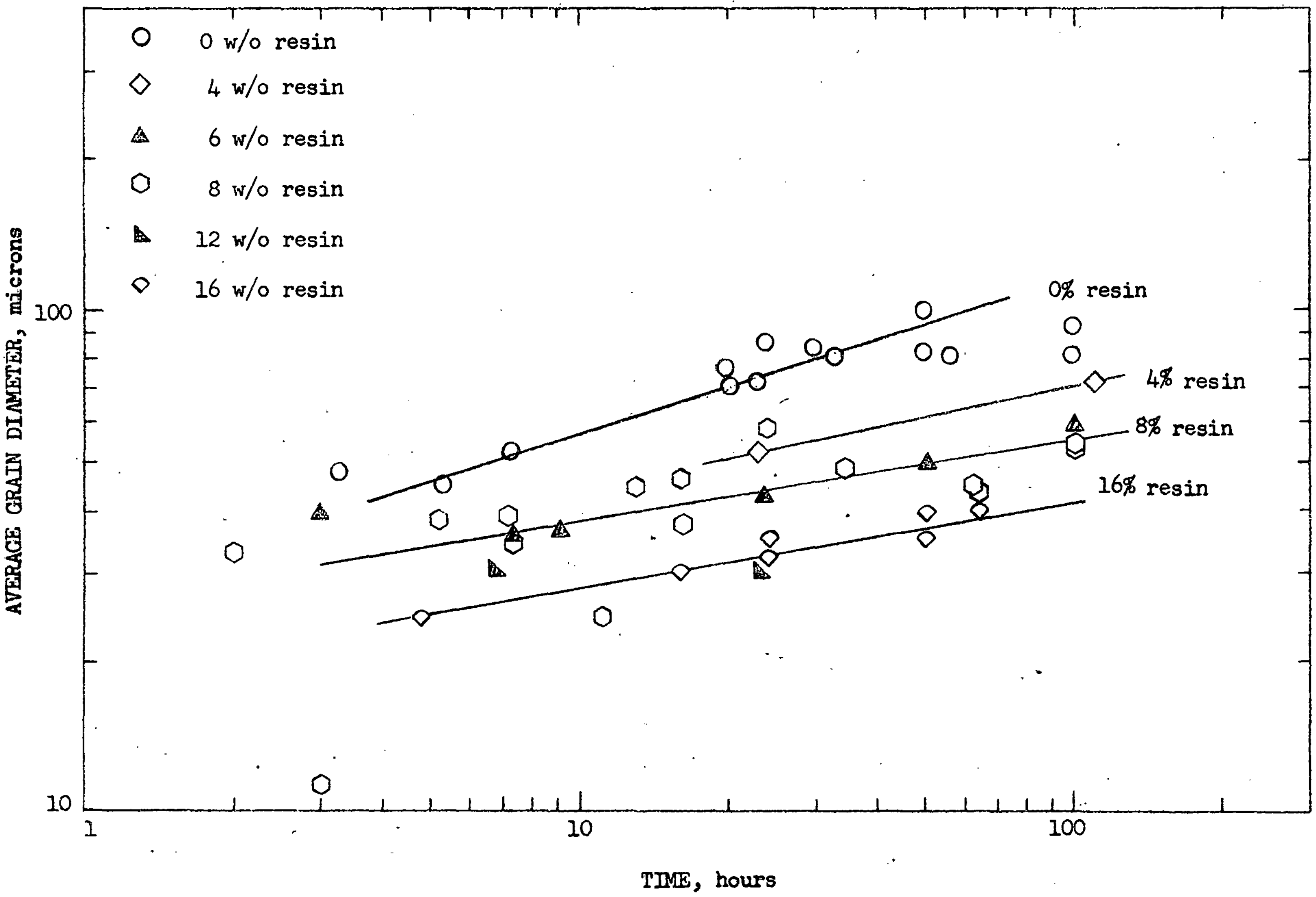

Fig. 17. Effect of additives on grain size of UOX grade BeO at 1500°C and 1700°C in hydrogen.

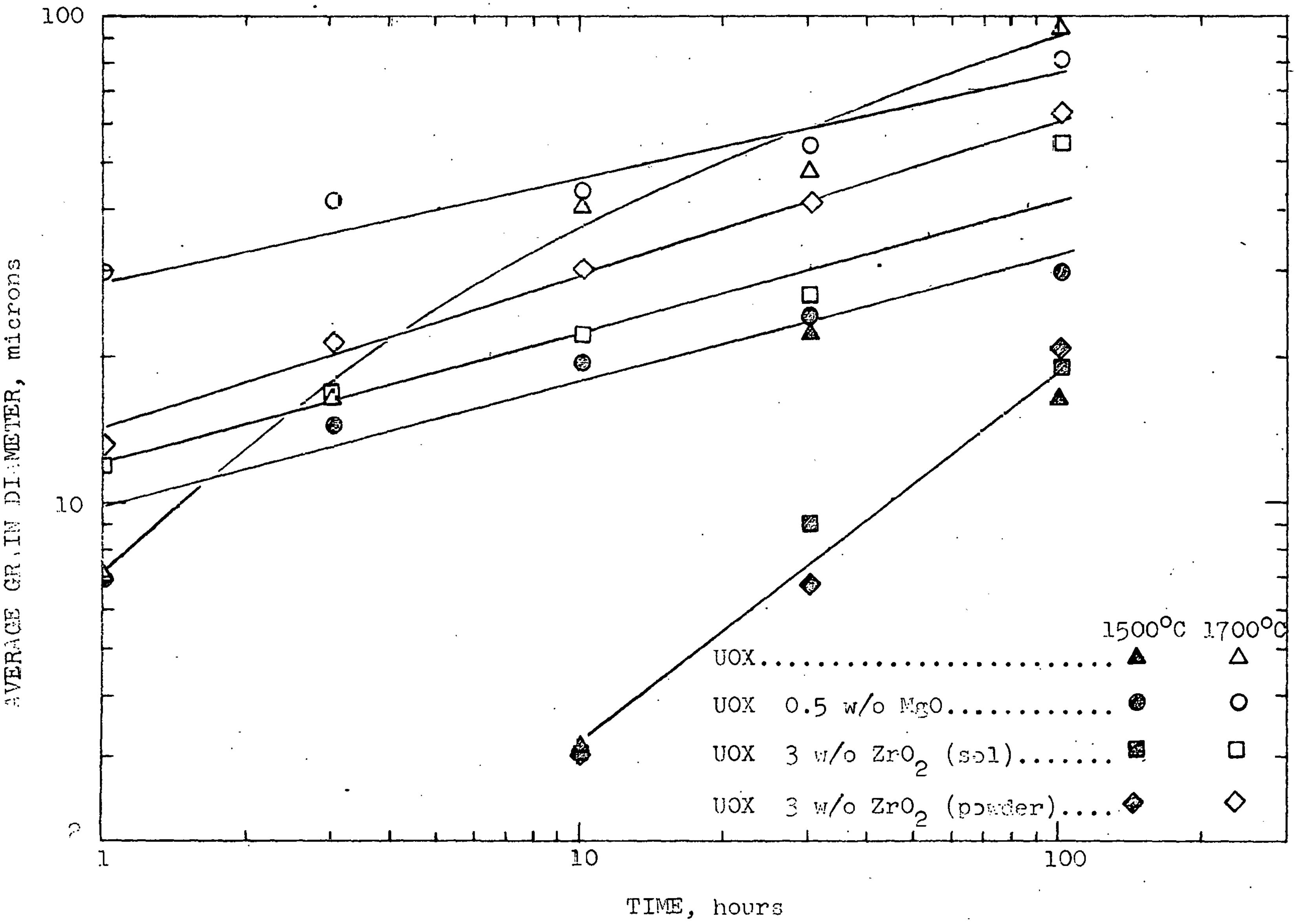

at which one would usually expect this type of growth to occur. many intragranular pores are observed in these relatively small grains. Felten (9c) made a similar observation with respect to grain growth rate and also attributed it to the occurrence of secondary growth.

A test which circumvents some of the complications introduced by densification was conducted in which sintered samples of UOX grade BeO, both with and withoug MgO and ZrO_2 additions and with approximately equal porosities and grain sizes, were given long time high temperature treatments in air. Density therefore remained practically constant throughout the test and only grain size changed. The results of this test at 1540°C in dry (-65°C dew point) air are given in Figure 18. Interpretation of these data is complicated by the fact that the grain size at the start of the test, D_o, is no longer small enough to be disregarded. Qualitatively, though, these data show that the grain growth rate of the UOX - ZrO_2 (sol) samples is definitely lower than that of the other samples.

Relationship Between Density and Grain Size

Figures 19 and 20 show the grain sizes and sintered densities of AOX and UOX + 0.5 w/o MgO samples, respectively, regardless of their sintering times or temperatures. The effect of changing the initial porosity of the samples by adding various quantities of minus 200 mesh phenolic resin or by calcining part of the AOX at 1290°C resulted in a lower final density. These curves are similar in shape to those given by Murray, Livey, and Williams (12)

Fig. 18. Grain size of UOX grade BeO with and without additives as a function of time at 1540°C in dry air. (At beginning of test, sintered densities ranged from approximately 96 to 99% of theoretical; grain sizes were as shown for 1 hour.)

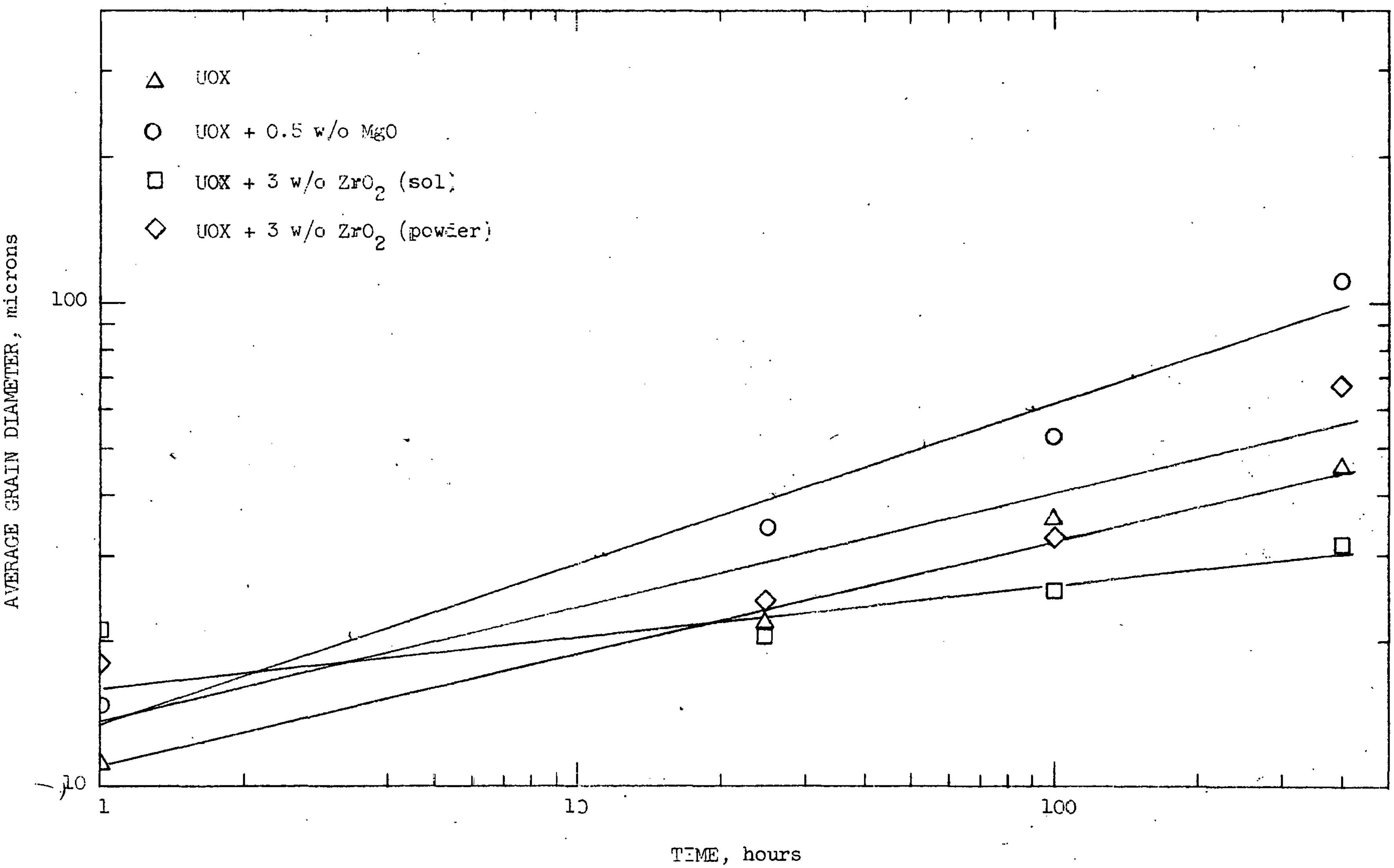

Fig. 19. Density - grain size relationship of AOX grade BeO and effect of resin additions.

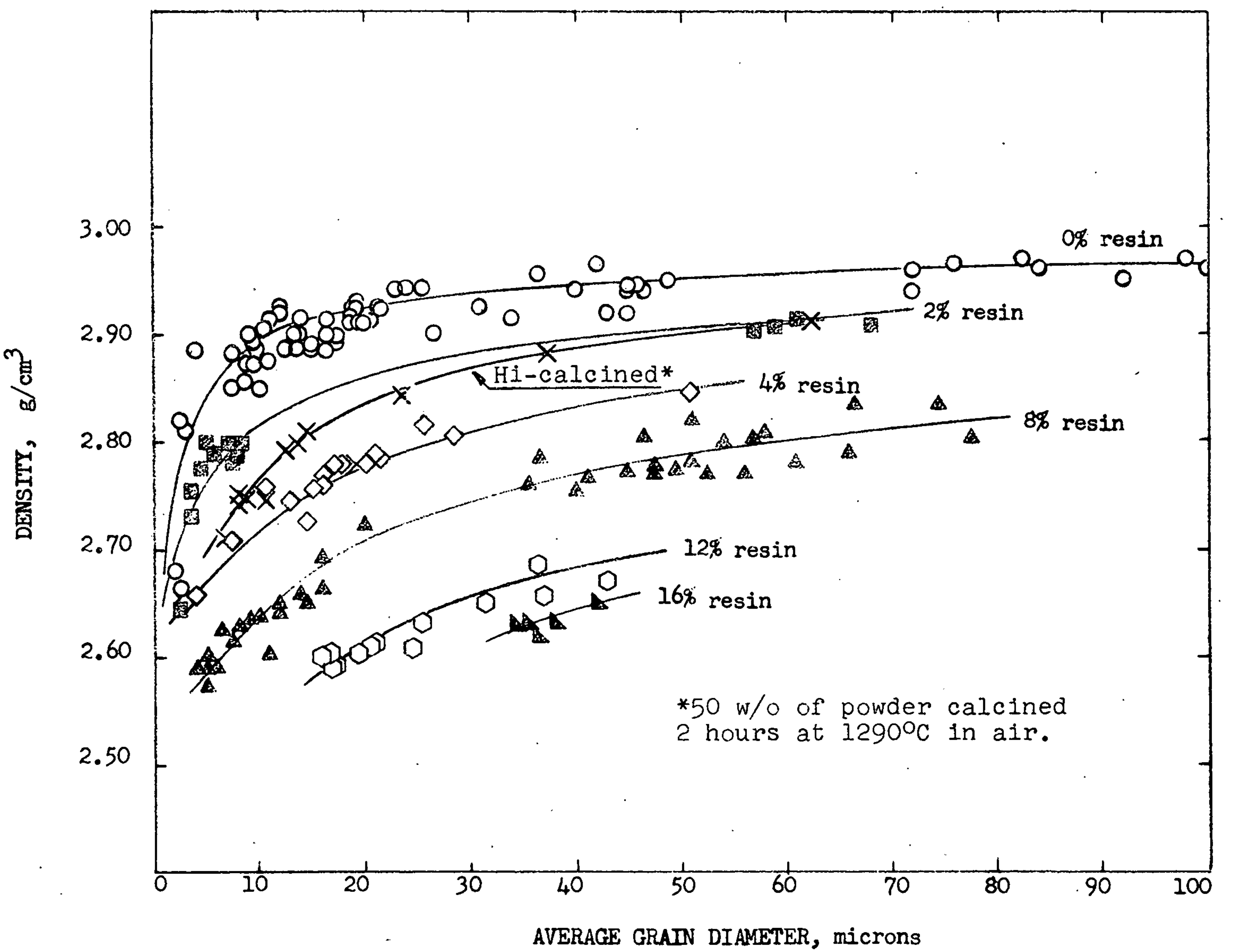

Fig. 20. Density - grain size relationship of UOX grade BeO + 0.5 w/o MgO and effect of resin additions.

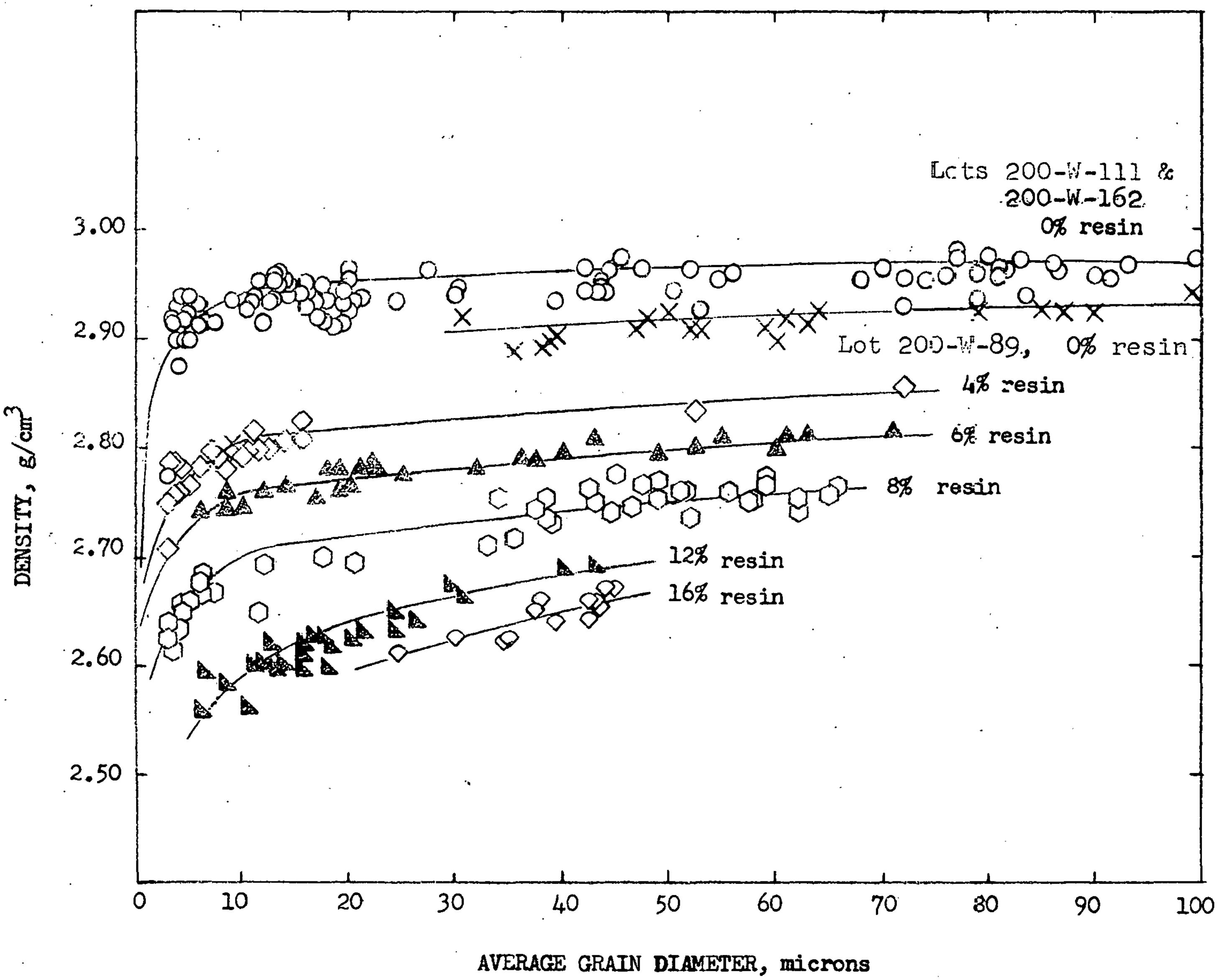

for sintered and hot-pressed BeO, and consistent with the observations of Bruch(13) on Al_2O_3.

CONCLUSIONS

It was possible to prepare irradiation test samples of BeO with varying densities, grain sizes and impurities. The most important conclusions from this work are as follows:

1. The sintering of the BeO samples prepared in this study followed the conventional sintering behavior with respect to density increase and grain growth as a function of time at temperature.

2. Low density samples could be prepared by the addition of an organic substance which volatilized during sintering, leaving pores of about 10 microns in diameter in the sintered piece. These pores were large enough to be unaffected by further heat treatment at the sintering temperature.

3. The desired microstructures were prepared by varying the sintering temperature and time at this temperature. It is to be noted, however, that grain growth at a given sintering temperature was observed to be decreased as the density was decreased, probably due to the relatively large pores produced by the resin additions.

4. The addition of 0.5 w/o MgO reduced the sintering temperature for 97% of theoretical density of high purity BeO (UOX and HPA grades) by about 200°C.

5. Some of the MgO used as a sintering aid was lost by volatilization during sintering in a hydrogen atmosphere.

The amount lost was dependent on the sintering temperature, the time at this temperature and the porosity of the sample.

6. The presence of large grains in the BeO powder used to prepare the samples retarded the sintering. Since these large grains were needle shaped they were aligned with the axis of extrusion. Also, since the "c" axis of the crystal was the long axis of these crystals, these extruded samples upon sintering showed enhanced preferred orientation with the "c" axes of the grains in the direction of extrusion.

REFERENCES

1. W.J. Kirkpatrick, G.R. Anderson, and E.S. Funston, "Basic Materials Studies Sinterable High Purity BeO, Final Report," GE-ANPD, APEX-684, 1961.

2. a) J.F. Quirk, N.B. Mosley, and W.H. Duckworth, "Characterization of Sinterable Oxide Powder: I, BeO," J. Am. Ceram. Soc., 40 (12) pp. 416-19, 1957.

   b) E.A. Aitken, "Initial Sintering Kinetics of Beryllium Oxide," J. Am. Ceram. Soc., 43 (12) pp. 627-33, 1960.

3. C.C. Browne, GE-NMPO, unpublished data.

4. a) L.H. Sjodahl and S.F. Bartram, "Preferred Orientation in Extruded BeO," GE-NMPO, TM 62-10-18, 1962.

   b) L.H. Sjodahl and S.F. Bartram, "Grain Orientation in Extruded BeO," GE-NMPO, TM 62-10-8, 1962.

5. a) First Annual Report - High-Temperature Materials and Reactor Component Development Programs, Vol. I-Materials, GE-NMPO, GEMP-106A, 1962.

5. b) High Temperature Materials Program Progress Report No. 12, Part A, GE-NMPO, GEMP-12A, 1962.

6. L. Navias, "Preparation and Properties of Spinel Made by Vapor Transport and Diffusion in the System $MgO-Al_2O_3$," J. Am. Ceram. Soc., 44 (9) pp. 434-46, 1961.

7. J.E. Burke, "Recrystallization and Sintering in Ceramics," pp. 120-31 in Ceramic Fabrication Processes, (W.D. Kingery, editor) Technology Press of Massachusetts Institute of Technology and John Wiley & Sons, Inc., New York, 1958.

8. J.E. Burke, "The Fundamentals of Recrystallization and Grain Growth," pp. 1-73 in Grain Control in Industrial Metallurgy, American Society for Metals, Cleveland, Ohio, 1949.

9. a) J.E. Burke, "Grain Growth in Ceramics," pp. 109-116 in Kinetics of High-Temperature Processes, (W.D. Kingery, editor), Tech. Press of Massachusetts Institute of Technology and John Wiley & Sons, Inc., New York, 1959.

b) R.L. Coble, "Sintering Crystalline Solids. II. Experimental Test of Diffusion Models in Powder Compacts," J. Appl. Phys., 32 (5) pp. 793-99, 1961.

c) E.J. Felten, "Sintering Behavior of Beryllium Oxide," J. Am. Ceramic Soc., 44 (6) pp. 251-55, 1961.

10. J.E. Burke and D. Turnbull, "Recrystallization and Grain Growth," pp. 220-92 in Progress in Metal Physics, Vol. III (Bruce Chalmers, editor) Interscience Publishers, Inc., New York, 1952.

11. I.B. Cutler, "Nucleation and Nuclei Growth in Sintered Alumina," pp. 120-27 in Kinetics of High Temperature Processes, (W.D. Kingery, editor) Technology Press of Massachusetts Institute of Technology and John Wiley and Sons, Inc., New York, 1959.

12. P. Murray, D.T. Livey, and J. Williams, "The Hot Pressing of Ceramics," pp. 147-71 in Ceramic Fabrication Processes, (W.D. Kingery, editor) Technology Press of Massachusetts Institute of Technology and John Wiley & Sons, Inc., New York, 1958.

13. C.A. Bruch, "Sintering Kinetics for the High Density Alumina Process," Am. Ceram. Soc. Bull., 41 (12) pp. 799-806, 1962.

ADVANCED TECHNOLOGY SERVICES

GENERAL ELECTRIC